Science of the Total Environment 954 (2024) 176243

Contents lists available at ScienceDirect

Science of the Total Environment

journal homepage: www.elsevier.com/locate/scitotenv

Tree stem-atmosphere greenhouse gas fluxes in a boreal riparian forest

Marcus Klaus [a,b,*], Mats Öquist [a], Kateřina Macháčová [b]

[a] Department of Forest Ecology and Management, Swedish University of Agricultural Sciences, Skogsmarksgränd 17, 90183 Umeå, Sweden
[b] Global Change Research Institute of the Czech Academy of Sciences, Bělidla 986/4a, 603 00 Brno, Czech Republic

HIGHLIGHTS

- Spatiotemporal variability of greenhouse gas fluxes in tree stems is understudied.
- We measured stem-atmosphere CO_2, CH_4 and N_2O fluxes in a boreal riparian forest.
- Stems emitted CO_2 and CH_4 with distinct spatiotemporal patters; N_2O fluxes were low.
- CO_2 and CH_4 emitted from stems originated likely from trees rather than soils.
- The studied forest acted like an upland system likely due to historic ditching.

GRAPHICAL ABSTRACT

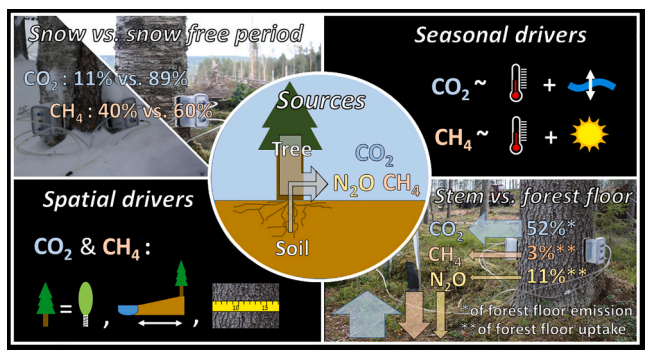

ARTICLE INFO

Editor: Charlotte Poschenrieder

Keywords:
Greenhouse gas emission
Spatiotemporal variability
Flux chamber
Bark
Forest floor
Laser spectrometer

ABSTRACT

Tree stems exchange greenhouse gases with the atmosphere but the magnitude, variability and drivers of these fluxes remain poorly understood. Here, we report stem fluxes of carbon dioxide (CO_2), methane (CH_4) and nitrous oxide (N_2O) in a boreal riparian forest, and investigate their spatiotemporal variability and ecosystem level importance. For two years, we measured CO_2 and CH_4 fluxes on a monthly basis in 14 spruces (*Picea abies*) and 14 birches (*Betula pendula*) growing near a headwater stream affected by historic ditching. We also measured N_2O fluxes on three occasions. All tree stems were net emitters of CO_2 and CH_4, while N_2O fluxes were around zero. CO_2 fluxes correlated strongly with air temperature and peaked in summer. CH_4 fluxes correlated modestly with air temperature and solar radiation and peaked in late winter and summer. Trees with larger stem diameter emitted more CO_2 and less CH_4 and trees closer to the stream emitted more CO_2 and CH_4. The CO_2 and CH_4 fluxes did not differ between spruce and birch, but correlations of CO_2 fluxes with stem diameter and distance to stream differed between the tree species. The absence of vertical trends in CO_2 and CH_4 fluxes along the stems and their low correlation with groundwater levels and soil CO_2 and CH_4 partial pressures suggest tree internal production as the primary source of stem emissions. At the ecosystem level, the stem CO_2, CH_4 and N_2O emissions represented 52 ± 16 % of the forest floor CO_2 emissions and 3 ± 1 % and 11 ± 40 % of the forest floor CH_4 and N_2O uptake, respectively, during the snow-free period (median ± SE). The six month snow-cover period contributed 11 ± 45 % and 40 ± 29 % to annual stem CO_2 and CH_4 emissions, respectively. Overall, the stem gas fluxes were more typical for upland rather than wetland ecosystems likely due to historic ditching and subsequent groundwater level decrease.

* Corresponding author at: Skogsmarksgränd 17, 90183 Umeå, Sweden.
E-mail address: marcus.klaus@slu.se (M. Klaus).

https://doi.org/10.1016/j.scitotenv.2024.176243
Received 4 June 2024; Received in revised form 22 August 2024; Accepted 11 September 2024
Available online 13 September 2024

1. Introduction

Rising atmospheric concentrations of the greenhouse gases (GHG) carbon dioxide (CO_2), methane (CH_4) and nitrous oxide (N_2O) arouse concerns about the cycling of these gases through ecosystems. However, our understanding of the global GHG cycle is limited by large uncertainties in the relative contributions of individual sources and sinks (Saunois et al., 2020). Forests are among the most important ecosystems in the global GHG cycle (Pan et al., 2011), exchanging CO_2, CH_4 and N_2O through leaves, branches, stems, ground vegetation and soil (Dalal and Allen, 2008). Tree stems are often neglected in forest GHG cycling studies despite decades of research on stem CO_2 exchange (Geurten, 1950; Teskey et al., 2008), and recent discoveries in stem CH_4 and N_2O exchange (Barba et al., 2019; Machacova et al., 2019). Many stems emit CO_2 and CH_4 with significant contribution to ecosystem scale budgets (Flanagan et al., 2021; Machacova et al., 2019; Pangala et al., 2017; Wang et al., 2016). Stem N_2O fluxes are usually low, but can be important under certain conditions (Machacova et al., 2019; Wen et al., 2017). Despite its importance, stem GHG exchange is generally not included in ecosystem and global GHG budgets (Covey and Megonigal, 2019; Friedlingstein et al., 2022; Saunois et al., 2020). Such efforts are severely challenged by the high complexity of underlying mechanisms and variability of fluxes in time and space (Barba et al., 2019).

In forest ecosystems, CO_2 is mainly produced by aerobic respiration and consumed by photosynthesis. CH_4 is mainly produced by methanogenesis under reducing conditions and consumed by methanotrophy under oxidizing conditions. N_2O is produced by several nitrogen turnover processes such as denitrification, nitrification-related pathways (including ammonium oxidation and nitrifier denitrification), and dissimilatory nitrate reduction to ammonium (cf. Hu et al., 2015). N_2O can also be consumed by denitrification, depending on redox conditions. In stems, GHGs are produced or consumed by microorganisms (Putkinen et al., 2021; Wang et al., 2016; Yip et al., 2019; Zeikus and Ward, 1974), photochemical processes (Jeffrey et al., 2021; Vigano et al., 2008), plant physiological processes (Keppler et al., 2006) or cryptogamic stem cover (Lenhart et al., 2015; Machacova et al., 2017). GHGs may also be produced in the soil and then transported via roots through the transpiration stream, intercellular spaces or air-filled aerenchyma into aboveground stem tissues via diffusion, pressurized ventilation or mass flow (Covey and Megonigal, 2019; Machacova et al., 2013; Maier et al., 2018; Rusch and Rennenberg, 1998; Teskey et al., 2008). Some studies also show CH_4 and N_2O uptake in stems through unknown mechanisms (Machacova et al., 2021; Sundqvist et al., 2012). In light of these variable mechanisms, there is still no general understanding of the extent to which GHGs in stems originate from trees or soils (Barba et al., 2024, 2019). This calls for a diversity of case studies performed in different ecosystems and under a wide range of environmental conditions that may favor one or the other mechanism.

A key challenge in determining the magnitudes and drivers of stem GHG fluxes is their high variability in time and space (Barba et al., 2024, 2019). Temporal variability has been attributed to temperature (Barba et al., 2021; Moldaschl et al., 2021; Pitz et al., 2018; Terazawa et al., 2015; Vainio et al., 2022), solar radiation (Machacova et al., 2019; Vigano et al., 2008), soil moisture and ground water level (Machacova et al., 2016; Pitz et al., 2018; Schindler et al., 2020), and/or soil GHG concentrations (Machacova et al., 2013; Pangala et al., 2015; Terazawa et al., 2015). Spatial variability has been attributed to tree species (Machacova et al., 2019, 2016; Pitz et al., 2018), diameter at breast height (dbh) (Pangala et al., 2015; Pitz and Megonigal, 2017; Wang et al., 2017) and general soil wetness (Moldaschl et al., 2021; Pitz and Megonigal, 2017). Most of these previous studies have focused on relatively short, subseasonal periods (Barba et al., 2021). Seasonal patterns, in particular the dormant winter period, remain largely unexplored, but could be significant for annual GHG budgets (Machacova et al., 2019; Mander et al., 2022; Ranniku et al., 2023). Spatial variability has typically been studied within relatively homogeneous ecosystems such as uplands or wetlands (Pitz and Megonigal, 2017). However, across ecosystems and their transition zones, patterns and drivers are particularly complex but remain poorly resolved (Barba et al., 2021; Terazawa et al., 2015). Hence, longer-term studies across different ecosystems are needed to expand the range of conditions that potentially shape temporal and spatial variation in stem GHG fluxes.

Riparian ecosystems, the interface between uplands and wetlands, cover 2 Mha globally (Tockner and Stanford, 2002) and exhibit particularly strong spatiotemporal variability in hydrological and biogeochemical conditions that promote hotspots of GHG cycling (McClain et al., 2003; Vidon et al., 2010). Studies from riparian ecosystems have been performed in hemiboreal, temperate and tropical biomes and show both emissions and uptake in stems (Flanagan et al., 2021; Mander et al., 2022, 2021; Moldaschl et al., 2021; Pitz et al., 2018; Schindler et al., 2020; Terazawa et al., 2021, 2015). However, these results cannot necessarily be transferred to other systems such as the boreal biome. In boreal riparian forests, GHG cycling can be expected to be particularly variable because of large seasonality in temperature and a dynamic snowmelt-dominated hydrological regime where GHGs in groundwater could be a potential source of stem GHG emissions (Schindler et al., 2020). Boreal riparian forests are abundant particularly along headwaters that cover a major proportion of the river networks (Laudon et al., 2022; Tockner and Stanford, 2002). Hence, boreal riparian zones provide an ideal setting to study patterns and drivers of stem GHG fluxes.

Many boreal riparian forests are subject to human activities that may modify GHG cycling. For example, many streams in Fennoscandia have been subject to ditch trenching to increase drainage aiding regeneration and forest productivity (Laudon et al., 2022). This has decreased groundwater levels with potential effects on soil redox conditions and GHG cycling (Laudon et al., 2023). Large parts of the world's boreal forests are managed and harvested by clear-cutting and an important conservation practice is to protect adjacent water bodies and wetlands from impacts of clear-cutting (Kuglerová et al., 2020). Therefore, a fringe of trees are usually left uncut, forming riparian buffer zones between clear-cuts and water bodies. Riparian buffer zones and ditching have been evaluated for their impact on many ecosystem services such as water or nutrient retention (Gundersen et al., 2010; Maher Hasselquist et al., 2021). However, the importance of riparian buffer zones and historic ditching for GHG fluxes in riparian forests, and stems in particular, is unknown (Laudon et al., 2023; Silverthorn and Richardson, 2021).

Here, we measured stem and forest floor fluxes of CO_2, CH_4 and N_2O in a riparian boreal forest buffer zone over two years. Our data had different temporal and spatial resolution for different gases and compartments and, accordingly, allowed us to explore (1) the magnitude and variability of stem fluxes of CO_2, CH_4 and N_2O; (2) the main drivers of stem CO_2 and CH_4 fluxes in time and space; (3) the potential origin of gas production; (4) the importance of the snow-cover period for annual stem CO_2 and CH_4 fluxes; and (5) the importance of stems relative to the forest floor for ecosystem scale CO_2, CH_4 and N_2O fluxes during the snow-free period. We test the following hypotheses:

H1. Tree species, dbh and distance to stream explain the spatial variation of stem CO_2 and CH_4 fluxes.

H2. Air temperature, solar radiation, groundwater level and soil CO_2 and CH_4 partial pressures (pCO_2, pCH_4) explain the temporal variation of stem CO_2 and CH_4 fluxes.

H3. If stem CO_2, CH_4 and N_2O emissions decrease with stem height, emissions may originate from CO_2, CH_4 and N_2O in soils. Additional support may be provided by a positive relationship between soil pCO_2 and pCH_4 or groundwater level, and stem CO_2 and CH_4 emissions, respectively.

H4. The snow-cover period contributes significantly to annual stem CO_2 and CH_4 fluxes.

H5. During the snow-free period, stem CO_2, CH_4 and N_2O fluxes can substantially contribute to ecosystem scale fluxes, such as forest floor fluxes.

Relative to published work, our study system is unique with respect to its high latitude and the riparian forest management history (Section 2.1). We therefore put high emphasis on discussing our findings in the context of other studies from boreal and hemiboreal upland, riparian and wetland forests and temperate riparian forests.

2. Materials and methods

2.1. Study site

The study was performed in a boreal riparian forest in northern Sweden (64.17°N, 19.84°E, 214–219 m.asl., Fig. 1)(Kuglerová et al., 2022). The area has a boreal humid climate with an annual temperature of 1.8 °C, annual precipitation of 614 mm (means during 1981–2010) and six month of snow cover (Laudon et al., 2013). Soils are characterized by nutrient poor podzol on glacial till. The forest is drained by a headwater stream that was trenched to ca. 1 m depth at some time between 1924 and 1939 (Norstedt, Gudrun, unpublished). On each side of the stream, riparian buffer zones of 5 m and 15 m width were created after the adjacent forest was clear-cut in February 2021 (Fig. 1b). The buffer widths are representative for Fennoscandia and North America (Kuglerová et al., 2020). Across the riparian buffer zone, organic layers decrease from 30–70 cm to 10–20 cm and mean groundwater tables increase from −70 to −50 cm with increased distance from the stream (Fig. S1). The riparian buffer zones consist mainly of Norway spruce (*Picea abies* (L.) H. Karst.), but also of silver birch (*Betula pendula* Roth) and a few Scotts pine (*Pinus sylvestris* L., Table S1). The tree species distribution is representative for Swedish riparian buffer zones (Maher Hasselquist et al., 2021). Tree ring inventories on stumps in the adjacent clear-cut suggest that most trees started growing in 1913. The ground vegetation was dominated by mosses (*Polytrichum* spp. Hedw., *Sphagnum* spp. L.) and dwarf shrubs (*Vaccinium myrtillus* L., *Vaccinium vitis-idaea* L.), a sparse cover of forbs (*Linnea borealis* L.), silver birch seedlings and several species of grasses. Tree bark was sparsely covered by cryptogams (average coverage <10 %, dominated by *Hypogymnia physodes* (L.) Nyl., *Parmeliopsis ambigua* (Wulfen) Nyl., and *Parmeliopsis hyperopta* (Ach.) Arnold) (Table S2).

2.2. Overview of the sampling program

Sampling was performed approximately monthly from May 2021 to May 2023 between 9 am and 4 pm, totaling 26 occasions. Sampling covered spring (March–May), summer (June–August), autumn (September–November) and winter (December–February). During spring snowmelt 2022, we sampled biweekly to capture flood dynamics. Snow conditions prevented us from sampling in December 2021 and January 2022. We avoided heavy rain to prevent damage to field equipment, but acknowledge their potential effect on stem GHG fluxes (Barba et al., 2021; Sakabe et al., 2021). During each field visit, we measured stem CO_2 and CH_4 fluxes. During the snow-free period (June–October), we also measured forest floor CO_2 and CH_4 fluxes within ±1 day of stem measurements. From February to October we sampled the soil gas atmosphere. During three occasions (June, August, October 2021), we measured stem and forest floor N_2O fluxes. We performed all calculations and statistical analyses using R v.4.3.1 (R Development Core Team, 2023).

2.3. Flux chamber design

We determined CO_2, CH_4 and N_2O fluxes using the closed static chamber method (non-vented, non-steady-state flow-through chambers) (Livingston and Hutchinson, 1995). We included 7 silver birch trees and

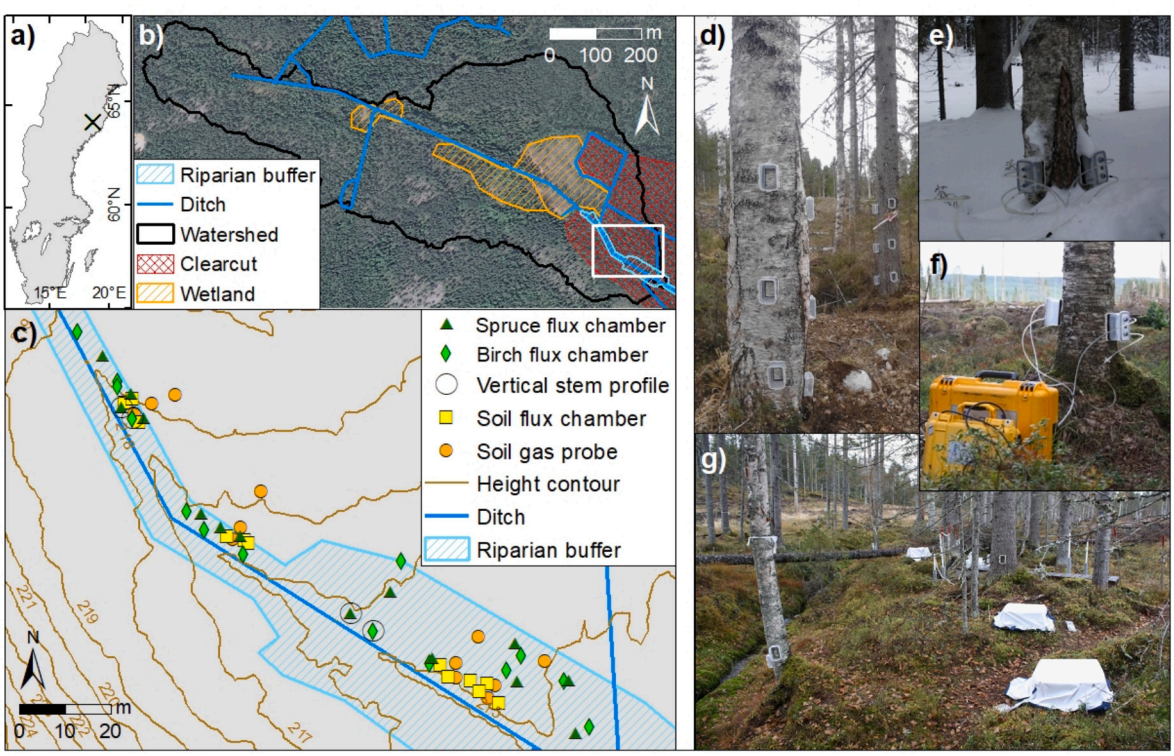

Fig. 1. Maps and photographs of the study site and sampling equipment. a) Location in Sweden, b) aerial photograph of the study area, taken before clearcutting, with land cover, 5 and 15 m wide riparian buffer zones and watershed delineation, c) flux chambers and soil gas probes, with height contours in m a.s.l.; the extent of the study area is marked by a white frame in b), d) stem flux chamber vertical profiles, e) winter and f) summer stem flux chamber measurements, g) forest floor flux chambers covered with opaque quilts to shut off photic processes.

7 Norway spruce trees in each buffer zone, totaling 28 trees (Fig. 1c). We selected all birches in the 5 and 15 m buffer zones, and for each birch, we selected a spruce within <8 m to reduce site-specific factors in species comparisons. On each tree, we installed two transparent stem chamber collars (Text S1) at 30–40 cm above ground at opposite sides (90–180° from each other) to capture radial variability (Barba et al., 2019). In four trees (one per species and buffer zone), we installed additional chamber pairs at 80–90 cm and 150–160 cm height to evaluate vertical trends and inform upscaling to whole trees (Fig. 1d). We measured forest floor fluxes at 12 plots within <24 m from the studied trees using transparent chambers (Text S1) covered with an opaque quilt to block out sunlight (Fig. 1c, g). Hence, forest floor measurements excluded photic processes, in contrast to the stem measurements. To account for this difference, we evaluated the effect of darkening on stem and forest floor CO_2 and CH_4 fluxes through additional campaigns (Text S2).

2.4. Flux measurements

We estimated CO_2 and CH_4 fluxes from respective concentration measurements inside the chamber pairs after closing them airtight with lids and interconnecting them in a closed loop (Fig. 1f). We measured the concentrations for 5–10 min (stems) and 5 min (forest floor) at 0.5 Hz using a laser spectrometer (Ultra-Portable GHG Analyzer, Los Gatos Research, San Jose, CA, USA). During each occasion, we measured all chambers on the same day following a fixed semi-randomized order, starting with the northern half of the 5 m buffer zone, then moving to the northern half of the 15 m buffer zone, the southern half of the 5 m buffer zone and finally the southern half of the 15 m buffer zone. This setup compromised between minimizing logistical efforts and assuring an equal distribution of daytimes across all trees/plots, even though diurnal variation in stem GHG fluxes is likely small in boreal/riparian forests (Mander et al., 2022; Schindler et al., 2021; Terazawa et al., 2015; Vainio et al., 2022).

We estimated stem and forest floor N_2O fluxes through manual sampling (Machacova et al., 2016). We sampled chamber air using a gas-tight syringe after flushing it with sample gas. We injected the samples into pre-evacuated 22 ml glass vials sealed with aluminum caps and butyl rubber stoppers. For the tree chambers, we took bulk samples (2 × 10 ml from each chamber of the same height level) at 1, 60, 120 and 180 min after closure. For forest floor chambers, we sampled 30 ml at 1, 15, 30 and 45 min after closure.

2.5. Soil gas sampling

We sampled soil gas using 24 soil gas probes (Text S3), located along four transects at distances of ~3, 6 and 16 m from the stream and at depths of 0.5–1 m and 0.7–1.3 m (Fig. 1c). We chose these depths to cover the Bs and C horizon, respectively, and the upper and lower end where fine roots are present (Fig. S8) and potentially take up GHGs from groundwater, the hypothesized main source of GHGs emitted from riparian trees (Sakabe et al., 2021). We sampled the gas probes by injecting 10 ml of ambient air through an inlet and simultaneously withdrawing 10 ml sample air through an outlet using two gas-tight syringes. We injected the sample air into evacuated glass vials that were pre-filled with 10 ml N_2.

2.6. Gas analysis

We analyzed soil probe and flux chamber gas samples on partial pressures pCO_2, pCH_4 and pN_2O within 1–2 weeks after sampling using a gas chromatograph (Clarus 580 with a Turbomatrix 110 Headspace autosampler, PerkinElmer, Shelton, CT, USA) by separation on an Elite-PLOT Q30m, 0.53mmID, 20 μm df column. Gases were separated at 30 °C using N_2 (10 psi) as carrier gas. CO_2 and CH_4 was detected with a Flame ionization detector containing a methanizer (350 °C, H_2 and air at 45 and 540 ml min^{-1}, respectively). N_2O was detected with an Electron capture detector (375 °C) with an Ar/CH_4 90 %/10 % mixture as make-up gas. The analytical accuracy was <5 % for all gases.

2.7. Ancillary data

We measured air temperature (T_a) and surface incoming shortwave solar radiation (SIS) every 30 min 1 km from our study site (64.175°N, 19.862°E, 186 m.asl.). We used a temperature probe in a 10-Plate Solar Radiation Shield (HC2S3 and 41003-5, Campbell Sci., Logan, UT, USA) and a net radiometer (NR01, Hukseflux, Delft, NL). We measured groundwater level (WL) and groundwater temperature (T_g) every hour using pressure data loggers (Levellogger® 5, Solinst Canada Ltd., Georgetown, CA) placed at the bottom of fully-screened high-density polyethylene wells (32 × 25 mm diameter, Unoson Environment AB, Mölnlycke, Sweden) extending 120 cm into the ground. We deployed four loggers, one in each soil gas probe transect at 3 m from the stream (Fig. 1c). We filled a few gaps in the time series data (Text S5). We also approximated groundwater levels manually during every field visit in 24 additional wells screened across the bottom 10 cm at the same locations and depths as the soil gas probes. During the snow-free period, we measured soil temperature (Digital Thermometer Model 3527A, Tsuruga Electric Corporation, Osaka, Japan) and soil moisture (ML3 ThetaProbe with a HH2 Soil Moisture Meter, Delta-T Devices Ltd., Cambridge, UK) at 5 cm depth at 10 cm distance from every side of the forest floor chamber collars. Soil temperature and moisture is often related to stem GHG fluxes (Barba et al., 2019) and here correlated strongly with continuously measured T_a and WL (ordinary least-squares linear regression, coefficient of determination $R^2 = 0.89$ and $R^2 = 0.66$, respectively, Fig. S3). We used the latter in further analyses because they were available for the full data record.

2.8. Flux calculations

We calculated the flux F between stems or the forest floor and the atmosphere using the R-package 'FluxCalR' (Zhao, 2019) as

$$F = V/(R \times T \times A) \times \Delta p/\Delta t \times \rho \quad (1)$$

where V is volume of the flux chamber including all tubings and the measurement cuvette of the analyzer, R is universal gas constant, T is ambient temperature, A is flux chamber basal area, $\Delta p/\Delta t$ is rate of gas partial pressure change over time t, and ρ is air pressure. $F > 0$ denotes gas emission to the atmosphere and $F < 0$ denotes uptake from the atmosphere. We computed $\Delta p/\Delta t$ using linear ordinary least squares regression. For CO_2 and CH_4, we used regression windows of 3–7 min. For N_2O, the regression included four manual samples. The mean ± SD R^2 for stem and forest floor fluxes was 0.96 ± 0.15 and 0.98 ± 0.03 for CO_2, 0.31 ± 0.30 and 0.86 ± 0.18 for CH_4, and 0.37 ± 0.33 and 0.42 ± 0.32 for N_2O respectively. We evaluated the quality of flux estimates using the minimum detectable flux (MDF) (Christiansen et al., 2015; Nickerson, 2016)

$$MDF = \frac{a}{t_c\sqrt{t_c/p_s}} V \Big/ (R \times T \times A) \times \rho \quad (2)$$

where a is analytical accuracy (300, 2 and 17 ppb for CO_2, CH_4 and N_2O, respectively), t_c is chamber closure time and p_s is sampling periodicity. The mean ± SD MDF for stem and forest floor fluxes was 0.39 ± 0.40 and 2.11 ± 0.74 nmol m^{-2} s^{-1} for CO_2, 2.50 ± 2.57 and 28 ± 7 pmol m^{-2} s^{-1} for CH_4, and 5.9 ± 1.4 and 38.7 ± 2.6 nmol m^{-2} s^{-1} for N_2O, respectively.

2.9. Analysis of environmental drivers

We evaluated environmental drivers of spatial and temporal variability in CO_2 and CH_4 fluxes by fitting a series of regression models

following standard procedures (Zuur et al., 2009). To evaluate drivers of spatial variability in gas fluxes among trees (H1), we fitted linear mixed effects models using the 'lme' function of the R package 'nlme' (Pinheiro and Bates, 2023). As fixed effects, we included tree species, dbh, distance to stream (d) and T_a. We also included three-way interactions of species and T_a with either dbh or d, and all respective two-way interactions, to explore expected differences in spatial patterns among tree species and throughout the year (Barba et al., 2021; Terazawa et al., 2015). As random effect, we included sampling occasion. Note that in this analysis, T_a effects relate to different time scales depending on whether it is included in interactions or as a single effect. In interaction with dbh and d, T_a reflects the effect of seasonal variation. As a single effect, T_a reflects the effect of diurnal variation. To meet assumptions on normality and homogeneity of residuals, we applied the signed square root transformation to fluxes and report original and back-transformed model parameters. We performed a reduction process to find the most parsimonious model, starting with the full model and removing stepwise the least significant fixed effect, prioritizing interactions, until model fits did not improve anymore. We evaluated models using Akaike Information Criterion (AIC), a measure of model fit relative to complexity.

We evaluated environmental drivers of temporal variability in CO_2 and CH_4 fluxes (H2) using generalized least squares regression. We performed this analysis based on stand-scale arithmetic mean values to acknowledge uncertainties in tree-specific environmental conditions that were not resolved here. We hypothesized temperature to be the main driver, based on biochemical kinetic theory (Yvon-Durocher et al., 2014), and hence fitted the data to an exponential model $F = j \times exp(k \times T_a)$, where j and k are parameters. We fitted this model separately for birch and spruce using the 'nls' function in R. We also report the proportional change of F for a 10 °C temperature increase $Q_{10} = exp(10k)$. We regressed the residuals of the F-T_a relationship against WL, T_g, SIS and pCO_2 or pCH_4 in the Bs horizon. We performed the regression using the 'gls' function from the R package 'nlme' (Pinheiro and Bates, 2023). In order to find the most parsimonious model, we fitted models with all possible combinations of predictors and ranked them based on AIC using the 'dredge' function from the R package 'MuMln' (Bartoń, 2023).

We evaluated the fits of the most parsimonious models by regressing observed against predicted values using ordinary least squares regression using the R function 'lm'. To characterize the fit of ordinary least square regression models, we report the R^2. For non-linear and generalized least square regressions we report the R^2 of the ordinary least square regression of observed vs. predicted values and denote it R^2_p. We tested for deviation of this regression from the 1:1 line as indicated by a significant intercept of this regression, and a significant slope of the regression of measured values minus predicted values vs. predicted values (Piñeiro et al., 2008). For mixed effects models, we report the fraction of variance explained by fixed effects (marginal R^2, R^2_m) and by fixed and random effects (conditional R^2, R^2_c), using the function 'r.squaredGLMM' of the R package 'MuMIn' (Bartoń, 2023). For details on model evaluation, see Text S6.

2.10. Vertical trends

To evaluate the origin of stem GHG emissions (H3), we assessed vertical trends with stem height. We fitted exponential regression models, assuming that fluxes decrease most rapidly with height near the ground (Mander et al., 2022; Sjögersten et al., 2020; Tarvainen et al., 2018; Vainio et al., 2022). We fitted $F = a \times exp(-b \times h)$, where h is height above ground and a and b are parameters. We fitted the model separately for birches and spruces using the 'nlme' function in the R package 'nlme' (Pinheiro and Bates, 2023), accounting for 'tree' as a random effect on a and b. Where necessary, we also accounted for serial correlation (Text S6). We did not find any clear seasonality in vertical trends and therefore lumped all data together.

2.11. Upscaling

We scaled stem area specific fluxes to the ecosystem ground area (Machacova et al., 2016), separately for birches and spruces and for the snow-free period (June-October) and the full year (H4). We assumed that near ground fluxes ($h = 0.35$ cm) were representative for the whole tree, because we did not find any exponential decrease with h (Section 3.3). We calculated ecosystem-scale stem fluxes per unit ground area as the product of the fluxes per unit stem area, the arithmetic mean stem area per tree, and the number of trees per hectare (Table S1). We calculated stem surface area using tree height and dbh, assuming a right circular cone shape. We calculated annual fluxes using a median, where each observation was weighted by the average number of days to the previous and consecutive sampling (Moldaschl et al., 2021). This procedure accounts for the variable sampling interval during the snow-cover period (26 ± 22 days). We calculated snow-free period fluxes using a regular median, because sampling occurred more regularly (32 ± 5 days). For the snow-free period, we compared ecosystem scale fluxes in stems and the forest floor (H5). We expressed forest floor fluxes per unit ground area after subtracting the stem basal area. Note that the upscaled fluxes generally refer to ambient light conditions during field sampling. For the 'ambient light' estimate, we multiplied forest floor fluxes measured under light exclusion by the average ratio of fluxes under ambient light and light exclusion (Fig. S4). For comparison, we also report CO_2 and CH_4 fluxes under light exclusion and regard the true annual flux to lie in between the reported boundaries. For the 'light exclusion' estimate, we multiplied stem fluxes measured under ambient light by the average ratio of fluxes under light exclusion and ambient light (Text S2, Fig. S7). We assume that these ratios are constant in space and time.

3. Results

3.1. Environmental conditions

Throughout the study, SIS varied from 0 to 800 W m^{-2}, T_a varied from −25 to 30 °C and T_g varied from 1.6 to 8.6 °C (Fig. 2). WL was as low as −1.17 m during winter base flow and as high as −0.04 m during floods. Snow was present between October and May and peaked at around 60 cm in April. Stem flux sampling covered the annual range in SIS, T_g and WL. Daytime sampling resulted in an overrepresentation of relatively well-lit and warm periods.

Soil pCO_2, pCH_4 and pN_2O varied from 6000 to 29,000 ppm, 0.8 to 8 ppm, and 0.1 to 10 ppm, respectively, as medians among sites, with highs during winter and summer and lows during spring and autumn (Fig. 2f–h). Relative to atmospheric levels, the soil was enriched in CO_2 and both enriched and depleted in CH_4. N_2O was near equilibrium in 2021 and enriched afterwards. Overall, the Bs and C horizon showed similar patterns. Variation between sites was similar (CO_2, N_2O) or larger (CH_4) than the seasonal variation of medians among sites. pCO_2 in the Bs and C horizon, and pN_2O in the Bs horizon decreased with distance to stream (Fig. S5). pCH_4 in the Bs and C horizon and pN_2O in the C horizon showed no relationship with distance to stream. 82 % of all soil gas samples were below the groundwater table at the time of sampling.

3.2. Stem and forest floor fluxes

We collected 1969 stem CO_2, CH_4 and N_2O flux estimates ($n = 911$, $n = 940$, $n = 108$) of which the majority showed emissions (98.4 %, 86.6 %, 56.5 %, respectively). CO_2 fluxes varied on a seasonal basis with highs of 2–3 μmol m^{-2} s^{-1} during mid-summer and lows of <0.1 μmol m^{-2} s^{-1} during mid-winter, as a median among individuals (Fig. 3a). CH_4 fluxes showed more complex patterns with highs of 0.05–0.1 nmol m^{-2} s^{-1} during spring and summer, and lows of ±0.02 nmol m^{-2} s^{-1} during autumn and winter (Fig. 3b). As a median across sampling dates, CO_2 emissions varied by a factor of five among individual trees. During

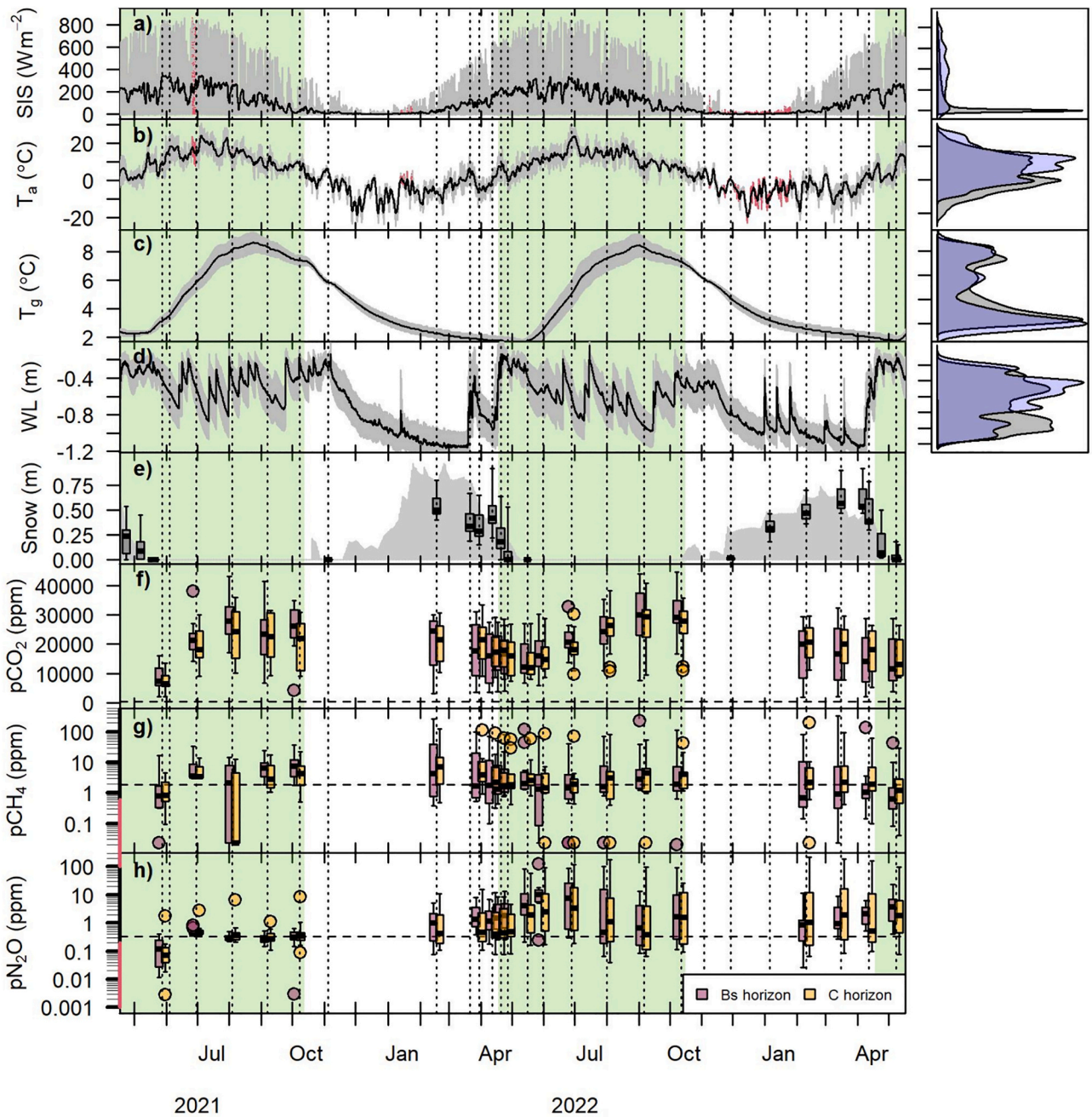

Fig. 2. Time series of environmental conditions. a) surface incoming shortwave solar radiation (SIS), b) air temperature (T_a), c) groundwater temperature above 1.2 m depth (T_g), d) groundwater level (WL), e) snow depth, f) soil pCO_2, g) soil pCH_4 and h) soil pN_2O. In a) and b) lines and grey shading show 2-day running means and 30 min measurements, respectively, and red shadings mark gap filled data. Lines and grey shading in c) and d) show means and SDs over 1 h measurements of four groundwater wells, respectively. Kernel density plots in a)–d) show frequency distributions of the whole study period (grey shading) and the sampling occasions (blue shading). Boxplots and grey shading in e) show measurements at the study site and daily recordings at the nearby (8.5 km) Svartberget research station, respectively. Boxplots in f)–h) show variability among all gas probes in the Bs and C horizon for each sampling occasion. Dashed horizontal lines mark the global average atmospheric gas partial pressure during 2021–2023 (Lan et al., 2024; Lan and Keeling, 2024). Red axis marking covers partial pressures outside the calibration interval. Green shading in all-time series plots mark the growing season (bound by first/last period of at least five consecutive days with mean $T_a > 5$ °C). Boxplots show medians (thick line), interquartile ranges (box), 1.5 times interquartile ranges (whiskers) and outliers (circles) among sampling sites. Boxplot location in f)–h) was jittered along the time axis per sampling occasion for better visibility.

the ten occasions when all trees emitted CH_4, the CH_4 emissions varied up to 27-fold among trees. In autumn and winter, CH_4 could be both taken up or emitted at 0.1 nmol m^{-2} s^{-1}. All CO_2 and CH_4 fluxes were above MDF. N_2O fluxes during the snow-free period 2021 averaged around 2 pmol m^{-2} s^{-1} with an approximate range of ±10 pmol m^{-2} s^{-1} (Fig. 3c). 0 %, 6 % and 63 % of all stem CO_2, CH_4 and N_2O fluxes, respectively, were below MDF.

The forest floor showed emissions of CO_2 and uptake of CH_4 during the snow-free period. The CO_2 fluxes showed highs of 2–6 μmol m^{-2} s^{-1} during mid-summer and lows of 1–2 μmol m^{-2} s^{-1} during spring and autumn, as a median among sampling sites (Fig. 3a). The CH_4 fluxes showed no clear seasonal pattern and ranged from −0.5 to −1.5 nmol m^{-2} s^{-1} (Fig. 3b). Fluxes varied 5-fold among sites for CO_2 and 6-fold for CH_4, as a median across sampling dates. Forest floor N_2O fluxes during

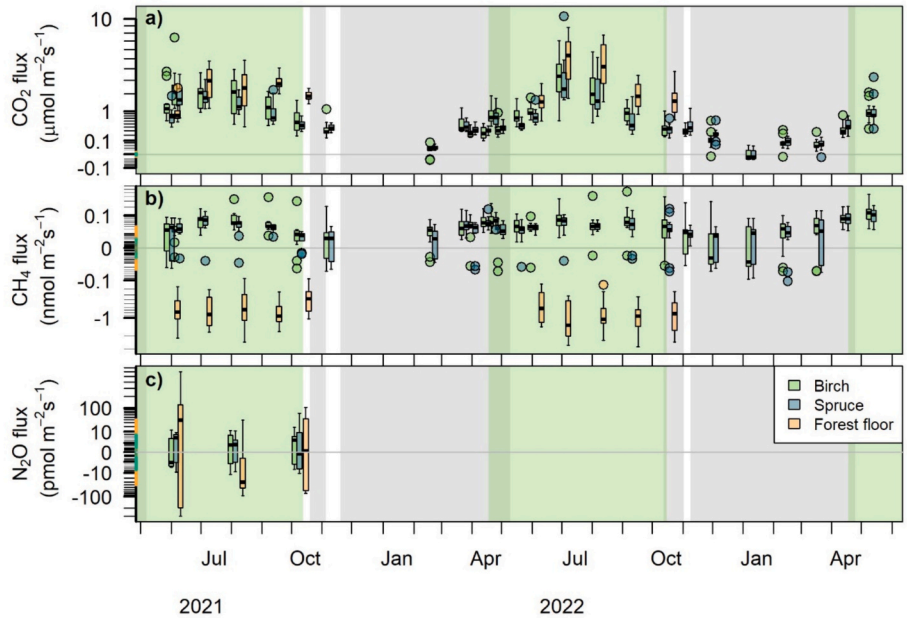

Fig. 3. Flux of CO_2 (a), CH_4 (b) and N_2O (c) in birch and spruce stems, as well as the forest floor, expressed per m^2 of stem area and forest floor, respectively. Boxplots show medians (thick line), interquartile ranges (box), 1.5 times interquartile ranges (whiskers) and outliers (circles) among sampling sites. Boxplot location was jittered along the time axis per sampling occasion for better visibility. Green shading shows the growing season. Grey shading shows the snow cover period. Dark green shading shows growing season with snow cover. Note the signed square root scale. Green and orange markings at the y-axis cover fluxes below the average MDF for stem and forest floor fluxes, respectively. Note that forest floor measurements represent darkened conditions and that N_2O fluxes were only measured during the growing season 2021.

the snow-free period averaged around −2 pmol m^{-2} s^{-1} with an approximate range of ±300 pmol m^{-2} s^{-1} (Fig. 3c). 0 %, 0 % and 46 % of all forest floor CO_2, CH_4 and N_2O fluxes, respectively, were below MDF.

3.3. Vertical trends in stem fluxes

The vertical profiles in GHG fluxes showed no consistent trend with height (Fig. 4) and generally, the nonlinear regression models did not yield any significant exponential trends (Table S3). An exception was CH_4 fluxes in birch that increased with height ($p = 0.02$). Yet, the exponential model had a poor fit ($R_p^2 = 0.16$), which we interpret as an absence of vertical trends.

3.4. Environmental drivers of spatial variations in stem fluxes

The CO_2 stem fluxes varied among trees depending on dbh and distance to stream (d) in interactions with tree species and T_a (Fig. 5a–d, Table S4). According to the model intercept that represents theoretical reference conditions ($T_a = 0$ °C, dbh = 0 cm, d = 1 m), birches and spruces emitted similar amounts of CO_2, 0.118 and 0.068 µmol m^{-2} s^{-1}, respectively (averages, here and onwards). For a 10 cm increase in dbh, CO_2 emissions increased by 0.035 µmol m^{-2} s^{-1} and 0.026 µmol m^{-2} s^{-1}, respectively. This dbh effect increased further by 0.024 µmol m^{-2} s^{-1} and decreased by 0.018 µmol m^{-2} s^{-1}, respectively, for a 10 °C increase in T_a. For a 10-fold increase in d, CO_2 emissions decreased by 0.063 µmol m^{-2} s^{-1} for birches, but increased by 0.094 µmol m^{-2} s^{-1} for spruces. This trend with d was independent of T_a in birches, but increased by 0.059 µmol m^{-2} s^{-1} in spruces for a 10 °C increase in T_a. Hence, higher temperatures generally amplified the spatial patterns of CO_2 fluxes. The model that described spatial patterns in CO_2 fluxes explained 49.9 % of variation and the fixed effects explained 45.7 %.

Stem CH_4 fluxes varied significantly among trees depending on dbh, d and T_a (Fig. 5e–h, Table S4). Birches and spruces emitted similar amounts of CH_4, 0.036 nmol m^{-2} s^{-1} at theoretical reference conditions.

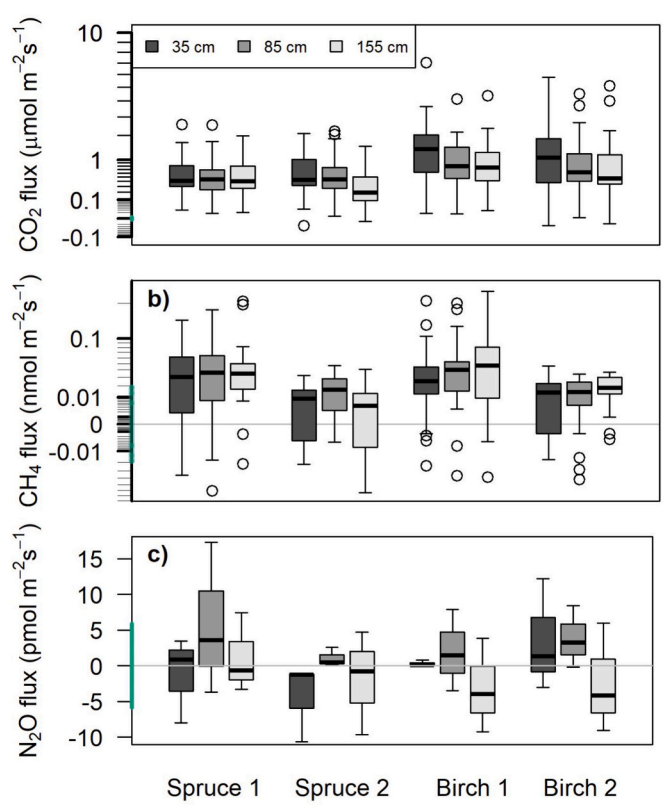

Fig. 4. Stem flux of CO_2 (a), CH_4 (b) and N_2O (c) as a function of height above ground for two spruces and birches. Boxplots show medians (thick line), interquartile ranges (box), 1.5 times interquartile ranges (whiskers) and outliers (circles) of 26 CO_2 and CH_4 sampling occasions and three N_2O sampling occasions. Green axis marking covers fluxes below the average MDF. Note the signed square root scale in a) and b).

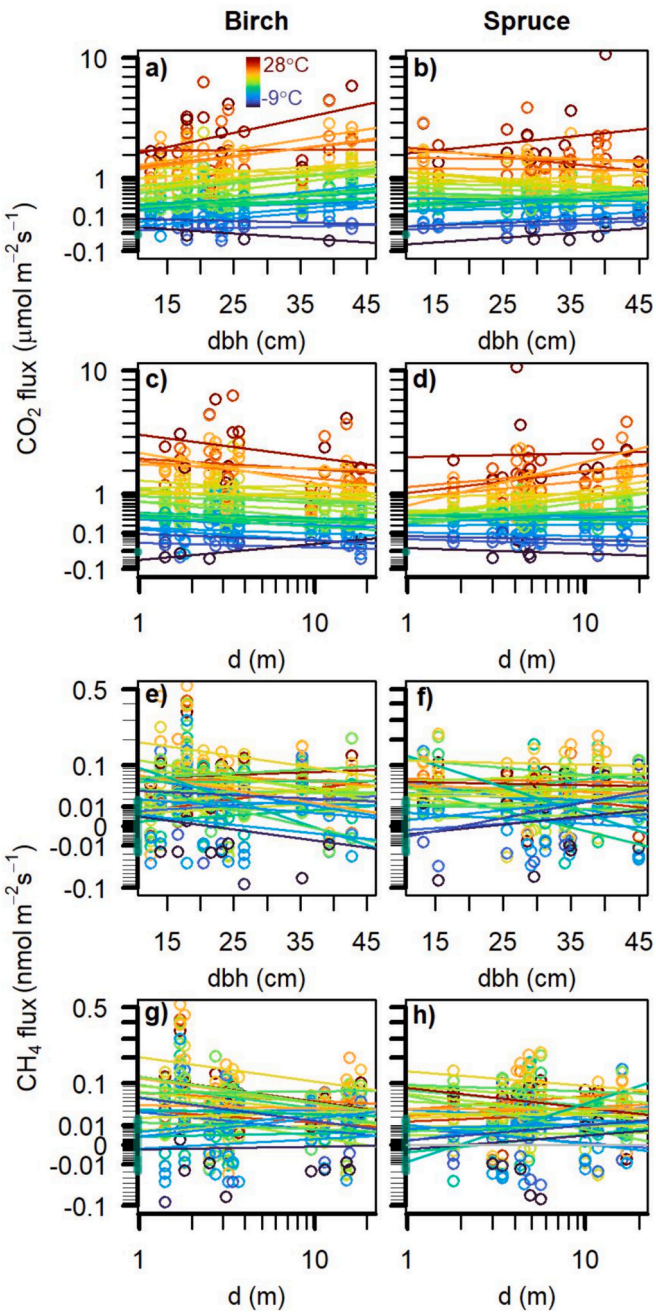

Fig. 5. Variation of stem CO_2 and CH_4 fluxes relative to diameter at breast height (dbh) and distance to stream (d) for birch and spruce. Circles show individual tree observations. The colored lines show linear regressions among individual trees for each sampling occasion with color gradient indicating mean air temperature. Green marking at the y-axis covers fluxes below the average MDF. Note the signed square root scale for CO_2 and CH_4 fluxes and the $\log_{10}$ scale for d.

For a 10 cm increase in dbh, CH_4 emissions decreased by 0.006 nmol m^{-2} s^{-1}. For a 10-fold increase in d, the CH_4 emissions decreased by 0.015 nmol m^{-2} s^{-1}. CH_4 emissions also increased by 0.018 nmol m^{-2} s^{-1} for a 10 °C increase in T_a. The model that described spatial patterns in CH_4 fluxes explained 6.5 % of variation and the fixed effects explained 2.2 %.

3.5. Environmental drivers of temporal variations in stem fluxes

Stand-scale average stem CO_2 and CH_4 fluxes increased exponentially with T_a (Fig. 6a, c). The CO_2 fluxes were more temperature sensitive than CH_4 fluxes in both birch and spruce, indicated by higher Q_{10} (2.45 vs. 1.39 and 2.54 vs. 1.45, respectively, Table S5) and better model fits ($R^2_p = 0.90$ vs. 0.23 and $R^2_p = 0.92$ vs. 0.21, respectively, Table S6). After accounting for T_a effects, the residual variation was best explained by linear effects of WL and SIS (Tables S7–S8). Residual CO_2 fluxes in birch and spruce increased by 0.18 and 0.23 µmol m^{-2} s^{-1}, respectively, for a 1 m WL rise, but the explained variance was low (Fig. 6b, $R^2_p = 0.06$ and $R^2_p = 0.04$, respectively). Residual CH_4 fluxes increased by 0.0073 and 0.0065 nmol m^{-2} s^{-1}, respectively, for a 100 W m^{-2} increase in SIS (Fig. 6d, $R^2_p = 0.11$ and $R^2_p = 0.30$, respectively). Soil pCO_2 and pCH_4 had negligible effects on stem fluxes (Table S7, Fig. S6).

3.6. Upscaling

During the six month long snow-free period, birches emitted 210 ± 68 kg CO_2-C ha^{-1}, 0.006 ± 0.003 kg CH_4-C ha^{-1} and 0.09 ± 0.43 g N_2O-N ha^{-1}, and spruces emitted 1084 ± 322 kg CO_2-C ha^{-1} yr^{-1}, 0.037 ± 0.009 kg CH_4-C ha^{-1} yr^{-1} and 3.25 ± 5.76 g N_2O-N ha^{-1} (weighted median ± standard error, expressed per forest ground area, Table 1). Birch and spruce stems together offset the CO_2 source and CH_4 and N_2O sink strength of the forest floor (equal to 100 %) by 52.1 ± 16.0 %, 2.5 ± 0.6 % and 11.3 ± 39.5 %, respectively. These numbers refer to ambient light conditions during our measurements and would deviate by up to 5–36 % under light exclusion (Table 1).

Spruce dominated over birch, with a contribution of 82–97 % to total birch and spruce stem CO_2, CH_4 and N_2O fluxes (Table 1), mainly because of their larger stand density and stem surface area (Table S1). The snow-free period contributed 83–95 % and 52–68 % to annual birch and spruce stem CO_2 and CH_4 emissions, respectively. Uncertainties in fluxes were large, especially for N_2O, as indicated by standard errors among individual trees and sampling occasions being 12–459 % of medians.

4. Discussion

4.1. Tree stems as emitters of CO_2 and CH_4

Stem GHG fluxes in our study showed many similarities, but also distinct differences to previous relevant studies because of its unique

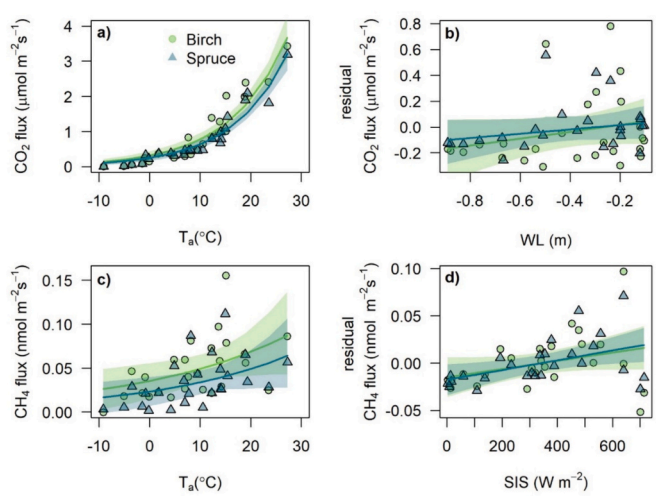

Fig. 6. Effect of environmental conditions on stem fluxes of CO_2 (a, b) and CH_4 (c, d). Shown are the primary exponential effects of air temperature (T_a) (a, c) and residual linear effects of groundwater level (WL, b) and surface incoming shortwave solar radiation (SIS, d). Points are stand-scale averages for each sampling occasion. Lines show regression fits and shadings show 95 % confidence intervals. The color code is consistent for points, lines and shadings.

Table 1
CO_2, CH_4 and N_2O fluxes for stems and the forest floor, upscaled to the ecosystem level and the snow-free and annual periods. Given are median ± standard error (SE) values of sampling occasion and tree-specific flux estimates, weighted by the average time in between consecutive samplings and using standard rules of error propagation. Hence, the error term of upscaled gas fluxes integrates variability among trees and over time. Fluxes are expressed per unit ground area and per sampling period (snow-free and annual). The relative contribution of period- or system specific fluxes to annual or total fluxes are also given for selected comparisons. Note that estimates generally refer to ambient light conditions during field sampling. For CO_2 and CH_4 fluxes estimates are also given for light exclusion conditions (in brackets), where appropriate (Text S2). No light exclusion data was available for N_2O fluxes and light exclusion effects were assumed to be negligible. NA is not available.

Period	System	CO_2		CH_4		N_2O	
		Median	SE	Median	SE	Median	SE
Ecosystem scale flux		kg C ha^{-1} period^{-1}		kg C ha^{-1} period^{-1}		g N ha^{-1} period^{-1}	
Snow free	Forest floor	2485 (3333)	427 (489)	−1.745 (−1.281)	0.209 (0.143)	−29.65	90.39
	Birch	210 (222)	68 (83)	0.006 (0.005)	0.003 (0.003)	0.09	0.43
	Spruce	1084 (1148)	322 (401)	0.037 (0.031)	0.009 (0.010)	3.25	5.76
Annual	Forest floor	NA	NA	NA	NA	NA	NA
	Birch	223 (236)	96 (110)	0.012 (0.010)	0.005 (0.005)	NA	NA
	Spruce	1300 (1376)	462 (551)	0.055 (0.046)	0.018 (0.017)	NA	NA

Period	System	CO_2		CH_4		N_2O	
		Median	SE	Median	SE	Median	SE
Relative contribution		%					
Snow free	Total tree: Forest floor	52.1 (41.1)	16.0 (13.7)	−2.5 (−2.9)	0.6 (0.9)	−11.3	39.5
	Spruce: Total tree	83.8	6.7	85.3	7.1	97.2	13.8
Annual	Spruce: Total tree	85.4	7.8	81.7	8.9	NA	NA
Snow free:Annual	Birch	94.5	51.0	52.1	30.8	NA	NA
	Spruce	83.4	38.6	68.2	27.5	NA	NA

setting in a managed boreal riparian buffer zone. We found that stems emitted CO_2 similar to previous boreal studies (Machacova et al., 2019; Marshall et al., 2023; Ogawa, 2006; Ryan et al., 1997; Shibistova et al., 2002; Stockfors and Linder, 1998) (Fig. 7a, b). Our stem CH_4 emission estimates were similar to many previous boreal or riparian studies (Machacova et al., 2016; Moldaschl et al., 2021; Ranniku et al., 2023; Vainio et al., 2022) (Fig. 7c, d), but lower than in several hemiboreal and temperate riparian studies (Flanagan et al., 2021; Mander et al., 2022; Sakabe et al., 2021; Terazawa et al., 2021, 2015). The relatively low CH_4 emissions in our site could be due to factors associated with the high latitude, such as the short growing season, or low soil fertility. It could also be due to the relatively short periods with groundwater levels near the soil surface (Fig. 2d), limiting the build-up of reducing conditions and hence CH_4 in soils as a potential source for stem emissions (Machacova et al., 2013). The stem CH_4 fluxes we found in winter were among the lowest reported in the literature and explained by relatively low temperatures and light conditions. Our CH_4 uptake estimate for the forest floor was of similar magnitude as in other upland or riparian forests (Flanagan et al., 2021; Machacova et al., 2016; Moldaschl et al., 2021; Vainio et al., 2022), but contrasted with lower uptake rates or even emissions in boreal or hemiboreal wetlands (Churkina et al., 2018; Mander et al., 2022; Ranniku et al., 2023; Terazawa et al., 2021; Vainio et al., 2022). Hence, the riparian zone acted more like an upland rather than a wetland system. This could be the consequence of historic ditching, followed by a groundwater level decline and an increase in the unsaturated zone where CH_4 can be efficiently oxidized. Experimental studies are needed to confirm this hypothesis.

We found that stem N_2O fluxes were low as characteristic for a nitrogen poor system such as our study area which receives an atmospheric deposition of ca. 2 kg N ha^{-1} year^{-1} (Laudon et al., 2023). Despite high uncertainties in individual flux estimates, averages indicated weak stem N_2O emissions. This is a common feature in boreal and riparian trees (Machacova et al., 2019, 2016; Moldaschl et al., 2021; Ranniku et al., 2023), even though flooding may enhance emissions beyond the range we measured (Mander et al., 2022) (Fig. 7e–f). The weak N_2O uptake of the forest floor in our study contrasted with N_2O emissions in other comparable studies (Machacova et al., 2019, 2016; Mander et al., 2021; Ranniku et al., 2023). This observation, together with high soil pN_2O relative to the atmosphere may suggest efficient N_2O consumption near the soil surface. However, upland forest soil near our study area were either very weak sinks or very weak sources of N_2O (Öquist et al., 2024). For more solid insights into N_2O fluxes and underlying mechanisms, high-frequency sampling is needed.

4.2. Spatial variation of stem fluxes and its drivers

The stem GHG fluxes in our study varied by several orders of magnitude. This is expected in riparian ecosystems because of strong spatial gradients and temporal variability in biogeochemical conditions (McClain et al., 2003; Vidon et al., 2010). The detailed patterns and drivers contrasted between CO_2 and CH_4, suggesting the processes involved in production and emission pathways are different (Barba et al., 2021). In particular, the patterns and drivers of CH_4 fluxes were less clear, compared to CO_2 fluxes. This can be expected since the net CH_4 flux involves both production and consumption pathways that typically are spatially separated according to the oxygen regime.

In partial agreement with hypothesis H1, variation in CO_2 and CH_4 fluxes among trees was related to dbh and d, but not to tree species. Thicker trees emitted more CO_2, likely because of their larger heartwood volume where gases can be produced, or their higher capacity to transport gases from the soil (Barba et al., 2021). This may be especially true for birches, which showed a larger dbh effect than spruces. CO_2 fluxes decreased for birches but increased for spruces the farther they were standing away from the stream. This may indicate that birches are morphologically and physiologically more adapted to growing near streams and their growth and associated respiration may benefit more from thicker near-stream organic layers and associated nutrients. Conversely, spruces may be more adapted to upland conditions, where they would occur more naturally than in riparian habitats (Maher Hasselquist et al., 2021). Interestingly, spatial patterns in CO_2 fluxes were amplified by higher T_a, indicating that temperature sensitivity depends on tree-specific traits (Ogawa, 2006). For example, thicker birches may have responded stronger to temperature because their growth and associated respiration was less restricted by other factors such as nutrient availability (Stockfors and Linder, 1998). Conversely, spruces farther from the stream may be less constrained by mal-

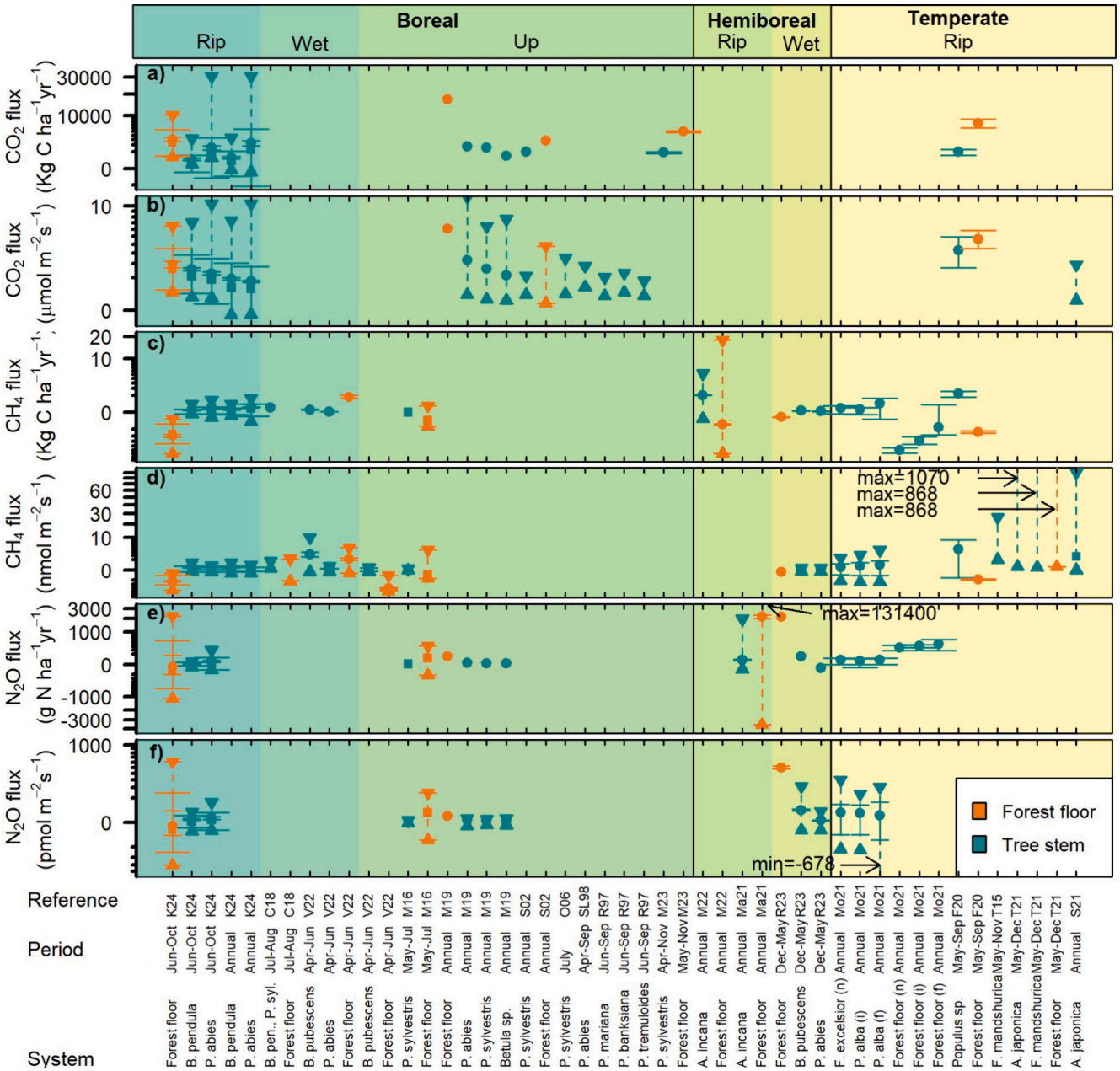

Fig. 7. Comparison of stem- and forest floor fluxes of CO_2 (a, b), CH_4 (c, d) and N_2O (e, f) in this study (K24) with other published studies from riparian ecosystems ('Rip') in the boreal, hemiboreal or temperate biome, and in addition, wetland or upland ecosystems ('Wet', 'Up') in the boreal and hemiboreal biome. Fluxes refer to the ecosystem scale per unit ground area (a, c, e) and the system-specific scale per unit stem or forest floor area (b, d, f). The abbreviations on the x-axis denote different studies and full references and source data are provided in Table S11. Note that the studies vary in many parameters, most importantly the period and tree species. Symbols show means (circles), medians (squares), standard deviations (solid error bars with wide ends), standard errors (solid error bars with narrow ends), minimum or maximum values (dashed error bars with triangle ends), as reported in the original papers. A is *Alnus* ssp., B is *Betula* ssp., F is *Fraxinus* ssp., P is *Picea* spp., *Pinus* ssp. or *Populus* ssp., respectively, n is non-flooded site, i is infrequently flooded site, f is flooded site.

adaptation to the riparian habitat. Integrated over the riparian zone, there was hence no difference in CO_2 emissions between birches and spruces, in agreement with a previous study across an upland-wetland gradient (Pitz et al., 2018).

The negative dbh effect on CH_4 fluxes both agrees and contrasts with previous findings from other ecosystems (Pangala et al., 2015; Pitz et al., 2018). This may be explained by a higher abundance of methanogens in thinner trees (Yip et al., 2019), but the exact mechanism remains unclear. Our finding of higher stem CH_4 emissions in the near-stream zone agrees with previous studies where it was explained by higher CH_4 uptake from soils under wetter conditions (Moldaschl et al., 2021; Pitz et al., 2018). The wetness effect is rather unlikely in our study, because groundwater levels were generally lower near the stream (Fig. S1b) and pCH_4 did not differ across the riparian zone (Fig. S5). We carefully suggest that in near-stream zones, the CH_4 emissions may have been stimulated by indirect effects of more nutrient-rich conditions on substrate quality and quantity relevant to stem-internal CH_4 production.

Spatial patterns of stem CH_4 fluxes were relatively weak and should be treated with caution. The low predictability may indicate that we underrepresented the spatiotemporal variability of predictor and predicted variables (Barba et al., 2021). For example, soil gases may vary more in space than we were able to resolve (Sakabe et al., 2021). Additionally, the range of predictor variables may have been too narrow. For example, the range of d was relatively small and the tree closest

to the stream was the only one located below the hillslope plateau, which had established after the stream was ditched (Fig. 1g). This birch showed the highest CH_4 emissions of all trees (outlier in Fig. 3b). Moreover, we may have missed other factors that are more directly related to the processes involved in CH_4 cycling such as microbial communities, sap flow or wood structure (Barba et al., 2019). Future studies should investigate morphological and physiological traits in order to resolve the mechanisms behind the spatial patterns found in our study.

4.3. Seasonal variation and its drivers

In line with hypothesis H2, stem CO_2 and CH_4 fluxes correlated with environmental conditions. The strong seasonality in CO_2 fluxes is a common feature and often explained by temperature effects on physiological processes such as stem respiration (Barba et al., 2021; Stockfors and Linder, 1998; Teskey et al., 2008). These dynamics are reflected by the exponential increase of stem CO_2 emissions with T_a. Our Q_{10} estimates were within the range reported for Scots pine (Ogawa, 2006; Tarvainen et al., 2018), but higher than values for Norway spruce (Stockfors and Linder, 1998) in upland forest stands 15 km away from our study site. This difference could be due to the wider range of temperatures included in our study. In particular, we found low but steady CO_2 emissions throughout the winter, likely as a result of low photosynthesis, transpiration and sap flow (Barba et al., 2021; Machacova et al., 2019; Pitz et al., 2018). Elevated CO_2 emissions during episodes with high groundwater levels (Fig. 6b) can potentially be due to many factors such as differences in respiration rates, wood diffusivity, sap flow or lenticel activity (Teskey et al., 2008), but further studies are needed to explain this.

Our stem CH_4 fluxes showed complex seasonal patterns, which are common (Barba et al., 2021; Machacova et al., 2023; Mander et al., 2022; Moldaschl et al., 2021; Pitz et al., 2018) and may indicate dependence on multiple factors and their interactions (Barba et al., 2021; Tenhovirta et al., 2022; Terazawa et al., 2015). For example, the relatively weak T_a effect on CH_4 fluxes in our study compared to many others (Barba et al., 2021; Moldaschl et al., 2021; Pangala et al., 2015; Pitz et al., 2018; Terazawa et al., 2021; Vainio et al., 2022) could have resulted from a negative correlation between T_a and soil moisture (Fig. S3c) and the partial cancellation of their individual effects (Mander et al., 2022). Interestingly, we detected considerable stem CH_4 emissions in late winter and spring, despite low temperatures (Fig. 3b). The relatively high CH_4 emissions could be a response of stems to freeze-thaw processes in order to avoid winter embolism (Lintunen et al., 2014), or to increased soil CH_4 accumulation as a result of limited gas exchange under the snow pack (Kim et al., 2012). Yet, if these were major factors, we would expect to see similar responses in CO_2 fluxes, which we did not. Alternatively, the relatively high CH_4 emissions could have been driven by the relatively high solar radiation, supported by the positive correlation between CH_4 fluxes and SIS (Fig. 6d). Solar radiation stimulates transpiration and may hence increase the vertical transport of CH_4 through the transpiration stream (Barba et al., 2019). This process is less likely here, because we observed high CH_4 emissions in both tree species before the onset of the growing season when transpiration can be expected to be rather low in spruce and negligible in birch before leaf out. Solar radiation also stimulates photosynthesis or other light-driven tree physiological processes, which in turn may enhance CH_4 production (Keppler et al., 2006; Tenhovirta et al., 2022; Vigano et al., 2008). The slight reduction in stem CH_4 emissions under dark conditions (Fig. S7, Table S9) could be a physiological response of cryptogamic stem covers. The cryptogams are known to exchange CH_4 with the atmosphere, even though previous studies have shown this flux to be independent of light conditions (Lenhart et al., 2015; Machacova et al., 2021). However, it remains open whether the light effect is limited to well-lit riparian buffer zones adjacent to clear-cuts or also apply to riparian forests with closed canopy. Clearly, the solar radiation effect warrants further investigation, e.g. through day-night time comparisons or more rigorous shading experiments.

4.4. Origin of the exchanged gases

Our findings fuel the ongoing debate on whether GHGs emitted from stems are primarily produced in the tree or the soil (Barba et al., 2019). In our study, stem GHG emissions have unlikely originated from soils for several reasons. *Firstly*, we did not observe any exponential decline in CO_2, CH_4 and N_2O fluxes with height above ground (Fig. 4). Previous boreal or riparian studies have shown a range of vertical trend patterns, suggesting that source contributions to stem fluxes is site- and tree-specific (Mander et al., 2022; Moldaschl et al., 2021; Ranniku et al., 2023; Vainio et al., 2022). *Secondly*, we found no or only weak correlations between stem CO_2 and CH_4 fluxes and groundwater levels or soil pCO_2 and pCH_4 (Fig. S6). In terms of CH_4, this observation could be explained by relatively low soil pCH_4 in our study and the relatively low groundwater levels and short flood durations, limiting soil CH_4 production and uptake through roots (Machacova et al., 2013; Moldaschl et al., 2021; Pitz et al., 2018). *Thirdly*, most of the roots were located in the upper aerated soil layers (Fig. S8) where pCH_4 was likely below atmospheric equilibrium as indicated by the consistent CH_4 uptake from the forest floor (Fig. 3b). *Fourthly*, if the soil was an important CO_2 and CH_4 source, we would expect higher emissions in birches because they usually root deeper than spruces and have higher sap flow rates, potentially leading to higher gas uptake from soils (Vainio et al., 2022). Species differences may also be expected because of differences in wood anatomy, affecting diffusive gas fluxes (Barba et al., 2019; Wang et al., 2016). *Fifthly*, we did not find any strong and consistent spatial trends of CO_2 and CH_4 fluxes with distance to stream that would support the soil origin hypothesis (Section 4.2).

We argue that the GHGs emitted from stems were primarily produced in the stem. While stem respiration, transport within the stem, and cryptogamic activity is generally regarded as the main source for CO_2 emissions (Teskey et al., 2008), the mechanism for CH_4 and N_2O production remains more uncertain. It is likely that CH_4 was produced by plant physiological processes (Keppler et al., 2006) or methanogenic archaea (Flanagan et al., 2021; Putkinen et al., 2021; Wang et al., 2016; Yip et al., 2019) or by cryptogams growing on the bark (Lenhart et al., 2015). N_2O production pathways may involve microbial production or various biotic and abiotic light dependent processes, but remain poorly understood (Machacova et al., 2019). We urge therefore for more mechanistic studies, including analysis of microbial composition, gas concentrations in stems and surface soil, stable isotopes and incubation studies (Barba et al., 2021; Flanagan et al., 2021; Wang et al., 2017; Yip et al., 2019).

It should be noted that we cannot fully rule out the soil-derived pathway for stem emissions. The missing correlation between stem fluxes and soil gas and groundwater level dynamics could be due to a mismatch between our soil gas sampling depths and the main rooting zone which is likely shallower (Puhe, 2003), or a time lag between environmental drivers and responses in microbial activity, soil gas production, root uptake and stem emission (Barba et al., 2024; Sakabe et al., 2021). Finally, our conclusions on the origin of N_2O must be treated with caution because of the limited quality and quantity of N_2O flux data. Nonetheless, our observations point towards internal GHG production pathways as the dominant source of stem emissions at the site.

4.5. Ecosystem level and annual importance

In partial support of hypothesis H4, stems emitted a significant amount of CO_2 relative to the forest floor (52.1 %), but were less important for CH_4 and N_2O fluxes (2.5 % and 11.3 %) at the ecosystem level. The contribution of stems to forest floor CO_2 fluxes in our study was higher than in other boreal studies or hemiboreal/temperate

riparian studies (16–42 %; (Flanagan et al., 2021; Machacova et al., 2019; Marshall et al., 2023; Shibistova et al., 2002)), mainly due to higher stand densities. The contribution of stems to forest floor CH_4 fluxes in our study was somewhat higher than in previous studies from relatively dry forests (~1 %, (Machacova et al., 2016; Moldaschl et al., 2021)) and lower than in flooded riparian forests (30 %–86 %, (Flanagan et al., 2021; Mander et al., 2022; Moldaschl et al., 2021)) and in wetland forests (14 %–22 %, (Ranniku et al., 2023; Vainio et al., 2022)). The contribution of stems to forest floor N_2O fluxes in our study was higher than in previous boreal or riparian studies (typically <2 %; (Machacova et al., 2019, 2016; Mander et al., 2021; Moldaschl et al., 2021; Ranniku et al., 2023)). Hence, our data supports the increasing evidence that stems cannot be ignored in ecosystem GHG budgets. To constrain the role of trees in ecosystem GHG fluxes further, significant gas exchange in branches, shoots and leaves should also be considered (Machacova et al., 2016; Mander et al., 2022; Vainio et al., 2022).

In support of hypothesis H5, the 6 month long snow cover period contributed significantly to the annual stem CO_2 and CH_4 emissions. Contributions to annual CO_2 emissions (11 %) were in the same range as reported for Scotts pine near our study site (Stockfors and Linder, 1998). Contributions for CH_4 were even higher in our study (40 %) and corroborates previous findings of non-negligible fluxes during snow cover (Mander et al., 2022; Ranniku et al., 2023). While we did not perform winter N_2O measurements, winter N_2O emissions from stems can be low but detectable in the boreal forest (Machacova et al., 2019). Therefore, the snow-cover period cannot be ignored in annual stem GHG budgets.

4.6. Conclusions

In summary, we show large spatiotemporal variability in the magnitudes and drivers of stem CO_2, CH_4 and N_2O fluxes in a boreal riparian forest buffer zone. Our results highlight the importance of weather conditions and tree specific traits for scaling up tree-level point measurements to annual and ecosystem-level estimates. The high variability and relatively poor predictability of GHG fluxes corroborates the increasingly recognized challenge behind the formulation of universal functional relationships needed for process-based modelling (Barba et al., 2021). Our data also suggest that stem GHG fluxes should be included in GHG budgets of riparian zones and that the snow-cover period should not be ignored. Finally, our study contributes to the ongoing debate on the origin of gases emitted from stems. We provide several lines of evidence that suggest trees rather than soils as the main source of GHGs emitted from stems. Hence, the riparian forest in our study acted more like an upland ecosystem where stem internal GHG production dominates (Covey et al., 2012; Wang et al., 2017) rather than a wetland ecosystem where gases are primarily soil derived (Pangala et al., 2015; Terazawa et al., 2021). We attribute this behavior to historical ditching, turning the former wetland-like forest into an upland-like system, and emphasize the need for experiments to test this hypothesis. Historical ditching is widespread in the boreal biome (Laudon et al., 2022) so that regional and global upscaling based on studies from more natural and wetter systems will likely overestimate gas emissions from riparian tree stems.

Supplementary data to this article can be found online at https://doi.org/10.1016/j.scitotenv.2024.176243.

CRediT authorship contribution statement

Marcus Klaus: Writing – original draft, Visualization, Software, Project administration, Methodology, Investigation, Funding acquisition, Formal analysis, Data curation, Conceptualization. **Mats Öquist:** Writing – review & editing, Supervision, Resources, Conceptualization. **Kateřina Macháčová:** Writing – review & editing, Resources, Methodology, Funding acquisition, Conceptualization.

Declaration of competing interest

The authors declare that they have no known competing financial interests or personal relationships that could have appeared to influence the work reported in this paper.

Data availability

Air temperature and solar radiation data is available upon request. All other data is available through the Trusted Digital Repository Swedish National Data Service (Klaus et al., 2024).

Acknowledgements

We thank Alice Falk, Elin Berg, Morgan Karlsson, Christer Moreira Boman, Hassan Ridha and the students of the Forest Ecosystem Ecology Master course 2021 and 2022 for field assistance. We also thank Jonas Lundholm, Meredith Blackburn, Abdul Mahomoud, Margareta Elfving and Jenny Ekman and the SLU Stable Isotope Laboratory (SSIL) and the Biogeochemical Analysis Laboratory (BAL) for lab analyses. We thank SITES Svartberget, Johannes Tiwari and Viktor Boström for logistical assistance. We thank Matthias Peichl for providing the gas analyzer and weather data, and Hjalmar Laudon for providing the field car. This work was supported by Stiftelsen Skogssällskapet (grant number 2019-657-Steg 2 2018), The Geological Survey of Sweden (grant number 36–2788/2021), Carl Tryggers Stiftelse (grant number CTS 20:226), Extensus Stiftelse and Stiftelsen Fonden för Skogsvetenskaplig Forskning. This work was further supported by project AdAgriF - Advanced methods of greenhouse gases emission reduction and sequestration in agriculture and forest landscape for climate change mitigation (CZ.02.01.01/00/22_008/0004635); The Ministry of Education, Youth and Sports of CR within the CzeCOS program (grant number LM2023048); and The Ministry of Education, Youth and Sports of CR within the LU - INTER-EXCELLENCE II (2022–2029) program (grant number LUC23162).

References

Barba, J., Bradford, M.A., Brewer, P.E., Bruhn, D., Covey, K., van Haren, J., Megonigal, J. P., Mikkelsen, T.N., Pangala, S.R., Pihlatie, M., Poulter, B., Rivas-Ubach, A., Schadt, C.W., Terazawa, K., Warner, D.L., Zhang, Z., Vargas, R., 2019. Methane emissions from tree stems: a new frontier in the global carbon cycle. New Phytol. 222, 18–28. https://doi.org/10.1111/nph.15582.

Barba, J., Poyatos, R., Capooci, M., Vargas, R., 2021. Spatiotemporal variability and origin of CO2 and CH4 tree stem fluxes in an upland forest. Glob. Chang. Biol. 27, 4879–4893. https://doi.org/10.1111/gcb.15783.

Barba, J., Brewer, P.E., Pangala, S.R., Machacova, K., 2024. Methane emissions from tree stems – current knowledge and challenges: an introduction to a virtual issue. New Phytol. 241, 1377–1380. https://doi.org/10.1111/nph.19512.

Bartoń, K., 2023. MuMIn: Multi-Model Inference (R package version 1.47.5).

Christiansen, J.R., Outhwaite, J., Smukler, S.M., 2015. Comparison of CO2, CH4 and N2O soil-atmosphere exchange measured in static chambers with cavity ring-down spectroscopy and gas chromatography. Agric. For. Meteorol. 211–212, 48–57. https://doi.org/10.1016/j.agrformet.2015.06.004.

Churkina, A.I., Mochenov, S.Y., Sabrekov, S.F., Glagolev, M.V., Il'Yasov, D.V., Terentieva, I.E., Maksyutov, S.S., 2018. Trees as methane sources: a case study of West Siberian South taiga. In: IOP Conference Series: Earth and Environmental Science 138. Institute of Physics Publishing. https://doi.org/10.1088/1755-1315/138/1/012002.

Covey, K.R., Megonigal, J.P., 2019. Methane production and emissions in trees and forests. New Phytol. https://doi.org/10.1111/nph.15624.

Covey, K.R., Wood, S.A., Warren II, R.J., Lee, X., Bradford, M.A., 2012. Elevated methane concentrations in trees of an upland forest. Geophys. Res. Lett. 39 https://doi.org/10.1029/2012GL052361.

Dalal, R.C., Allen, D.E., 2008. Turner review no. 18. Greenhouse gas fluxes from natural ecosystems. Aust. J. Bot. 56, 369–407. https://doi.org/10.1071/BT07128.

Flanagan, L.B., Nikkel, D.J., Scherloski, L.M., Tkach, R.E., Smits, K.M., Selinger, L.B., Rood, S.B., 2021. Multiple processes contribute to methane emission in a riparian cottonwood forest ecosystem. New Phytol. 229, 1970–1982. https://doi.org/10.1111/nph.16977.

Friedlingstein, P., Jones, M.W., Sullivan, M.O., Andrew, R.M., Bakker, D.C.E., Hauck, J., Quéré, C. Le, Peters, G.P., Peters, W., 2022. Global carbon budget 2021. Earth Syst Sci Data 14, 1917–2005. https://doi.org/10.5194/essd-14-1917-2022.

Geurten, I., 1950. Untersuchungen über den Gaswechsel von Baumrinden. Forstwissenschaftliches Centralblatt 69, 704–743. https://doi.org/10.1007/BF01973815.

Gundersen, P., Laurén, A., Finér, L., Ring, E., Koivusalo, H., Sætersdal, M., Weslien, J.O., Sigurdsson, B.D., Högbom, L., Laine, J., Hansen, K., 2010. Environmental services provided from riparian forests in the nordic countries. Ambio 39, 555–566. https://doi.org/10.1007/s13280-010-0073-9.

Hu, H.W., Chen, D., He, J.Z., 2015. Microbial regulation of terrestrial nitrous oxide formation: understanding the biological pathways for prediction of emission rates. FEMS Microbiol. Rev. https://doi.org/10.1093/femsre/fuv021.

Jeffrey, L.C., Maher, D.T., Tait, D.R., Reading, M.J., Chiri, E., Greening, C., Johnston, S. G., 2021. Isotopic evidence for axial tree stem methane oxidation within subtropical lowland forests. New Phytol. 230, 2200–2212. https://doi.org/10.1111/nph.17343.

Keppler, F., Hamilton, J.T.G., Braß, M., Röckmann, T., 2006. Methane emissions from terrestrial plants under aerobic conditions. Nature 439, 187–191. https://doi.org/10.1038/nature04420.

Kim, D.G., Vargas, R., Bond-Lamberty, B., Turetsky, M.R., 2012. Effects of soil rewetting and thawing on soil gas fluxes: a review of current literature and suggestions for future research. Biogeosciences 9, 2459–2483. https://doi.org/10.5194/bg-9-2459-2012.

Klaus, M., Öquist, M., Machacova, K., 2024. Tree Stem-atmosphere Greenhouse Gas Fluxes in a Boreal Riparian Forest (Version 1) [Data set]. Swedish National Data Service. https://snd.se/en/catalogue/dataset/preview/bb4db99d-8386-4d83-bb93-58136f590dcd/1 [WWW Document]. https://doi.org/10.5878/9jqq-s279.

Kuglerová, L., Jyväsjärvi, J., Ruffing, C., Muotka, T., Jonsson, A., Andersson, E., Richardson, J.S., 2020. Cutting edge: a comparison of contemporary practices of riparian buffer retention around small streams in Canada, Finland, and Sweden. Water Resour. Res. 56 https://doi.org/10.1029/2019WR026381.

Kuglerová, L., Nilsson, G., Hasselquist, E.M., 2022. Too much, too soon? Two Swedish case studies of short-term deadwood recruitment in riparian buffers. Ambio 52, 440–452. https://doi.org/10.1007/s13280.

Lan, X., Keeling, R., 2024. Trends in Atmospheric Carbon Dioxide [WWW Document]. URL. https://gml.noaa.gov/ccgg/trends/data.html (accessed 3.18.24).

Lan, X., Thoning, K.W., Dlugokencky, E.J., 2024. Trends in Globally-averaged CH4, N2O, and SF6 Determined From NOAA Global Monitoring Laboratory Measurements. Version 2024-03 [WWW Document]. https://doi.org/10.15138/P8XG-AA10.

Laudon, H., Taberman, I., Ågren, A., Futter, M., Ottosson-Löfvenius, M., Bishop, K., 2013. The Krycklan Catchment Study - a flagship infrastructure for hydrology, biogeochemistry, and climate research in the boreal landscape. Water Resour. Res. 49, 7154–7158. https://doi.org/10.1002/wrcr.20520.

Laudon, H., Lidberg, W., Sponseller, R.A., Maher Hasselquist, E., Westphal, F., Östlund, L., Sandström, C., Järveoja, J., Peichl, M., Ågren, A.M., 2022. Emerging technology can guide ecosystem restoration for future water security. Hydrol. Process. 36 https://doi.org/10.1002/hyp.14729.

Laudon, H., Mosquera, V., Eklöf, K., Järveoja, J., Karimi, S., Krasnova, A., Peichl, M., Pinkwart, A., Tong, C.H.M., Wallin, M.B., Zannella, A., Hasselquist, E.M., 2023. Consequences of rewetting and ditch cleaning on hydrology, water quality and greenhouse gas balance in a drained northern landscape. Sci. Rep. 13 https://doi.org/10.1038/s41598-023-47528-4.

Lenhart, K., Weber, B., Elbert, W., Steinkamp, J., Clough, T., Crutzen, P., Pöschl, U., Keppler, F., 2015. Nitrous oxide and methane emissions from cryptogamic covers. Glob. Chang. Biol. 21, 3889–3900. https://doi.org/10.1111/gcb.12995.

Lintunen, A., Lindfors, L., Kolari, P., Juurola, E., Nikinmaa, E., Hölttä, T., 2014. Bursts of CO_2 released during freezing offer a new perspective on avoidance of winter embolism in trees. Ann. Bot. 114, 1711–1718. https://doi.org/10.1093/aob/mcul90.

Livingston, G.P., Hutchinson, G.L., 1995. Enclosure-based measurement of trace gas exchange: applications and sources of error. In: Biogenic Trace Gases: Measuring Emissions from Soil and Water, pp. 14–51.

Machacova, K., Papen, H., Kreuzwieser, J., Rennenberg, H., 2013. Inundation strongly stimulates nitrous oxide emissions from stems of the upland tree Fagus sylvatica and the riparian tree Alnus glutinosa. Plant and Soil 364, 287–301. https://doi.org/10.1007/s11104-012-1359-4.

Machacova, K., Bäck, J., Vanhatalo, A., Halmeenmäki, E., Kolari, P., Mammarella, I., Pumpanen, J., Acosta, M., Urban, O., Pihlatie, M., 2016. Pinus sylvestris as a missing source of nitrous oxide and methane in boreal forest. Sci. Rep. 6 https://doi.org/10.1038/srep23410.

Machacova, K., Maier, M., Svobodova, K., Lang, F., Urban, O., 2017. Cryptogamic stem covers may contribute to nitrous oxide consumption by mature beech trees. Sci. Rep. 7 https://doi.org/10.1038/s41598-017-13781-7.

Machacova, K., Vainio, E., Urban, O., Pihlatie, M., 2019. Seasonal dynamics of stem N2O exchange follow the physiological activity of boreal trees. Nat. Commun. 10 https://doi.org/10.1038/s41467-019-12976-y.

Machacova, K., Borak, L., Agyei, T., Schindler, T., Soosaar, K., Mander, Ü., Ah-Peng, C., 2021. Trees as net sinks for methane (CH4) and nitrous oxide (N2O) in the lowland tropical rain forest on volcanic Réunion Island. New Phytol. 229, 1983–1994. https://doi.org/10.1111/nph.17002.

Machacova, K., Warlo, H., Svobodová, K., Agyei, T., Uchytilová, T., Horáček, P., Lang, F., 2023. Methane emission from stems of European beech (Fagus sylvatica) offsets as much as half of methane oxidation in soil. New Phytol. 238, 584–597. https://doi.org/10.1111/nph.18726.

Maher Hasselquist, E., Kuglerová, L., Sjögren, J., Hjältén, J., Ring, E., Sponseller, R.A., Andersson, E., Lundström, J., Mancheva, I., Nordin, A., Laudon, H., 2021. Moving towards multi-layered, mixed-species forests in riparian buffers will enhance their long-term function in boreal landscapes. For. Ecol. Manage. 493, 119254 https://doi.org/10.1016/j.foreco.2021.119254.

Maier, M., Machacova, K., Lang, F., Svobodova, K., Urban, O., 2018. Combining soil and tree-stem flux measurements and soil gas profiles to understand CH4 pathways in Fagus sylvatica forests. J. Plant Nutr. Soil Sci. 181, 31–35. https://doi.org/10.1002/jpln.201600405.

Mander, Ü., Krasnova, A., Escuer-Gatius, J., Espenberg, M., Schindler, T., Machacova, K., Pärn, J., Maddison, M., Megonigal, J.P., Pihlatie, M., Kasak, K., Niinemets, Ü., Junninen, H., Soosaar, K., 2021. Forest canopy mitigates soil N2O emission during hot moments. NPJ Clim Atmos Sci 4, 39. https://doi.org/10.1038/s41612-021-00194-7.

Mander, Ü., Krasnova, A., Schindler, T., Megonigal, J.P., Escuer-Gatius, J., Espenberg, M., Machacova, K., Maddison, M., Pärn, J., Ranniku, R., Pihlatie, M., Kasak, K., Niinemets, Ü., Soosaar, K., 2022. Long-term dynamics of soil, tree stem and ecosystem methane fluxes in a riparian forest. Sci. Total Environ. 809, 151723 https://doi.org/10.1016/j.scitotenv.2021.151723.

Marshall, J.D., Tarvainen, L., Zhao, P., Lim, H., Wallin, G., Näsholm, T., Lundmark, T., Linder, S., Peichl, M., 2023. Components explain, but do eddy fluxes constrain? Carbon budget of a nitrogen-fertilized boreal Scots pine forest. New Phytol. 239, 2166–2179. https://doi.org/10.1111/nph.18939.

McClain, M.E., Boyer, E.W., Dent, C.L., Gergel, S.E., Grimm, N.B., Groffman, P.M., Hart, S.C., Harvey, J.W., Johnston, C.A., Mayorga, E., McDowell, W.H., Pinay, G., 2003. Biogeochemical hot spots and hot moments at the interface of terrestrial and aquatic ecosystems. Ecosystems 6, 301–312. https://doi.org/10.1007/s10021-003-0161-9.

Moldaschl, E., Kitzler, B., Machacova, K., Schindler, T., Schindlbacher, A., 2021. Stem CH4 and N2O fluxes of Fraxinus excelsior and Populus alba trees along a flooding gradient. Plant and Soil 461, 407–420. https://doi.org/10.1007/s11104-020-04818-4.

Nickerson, N., 2016. Evaluating Gas Emission Measurements Using Minimum Detectable Flux (MDF). https://doi.org/10.13140/RG.2.1.4149.2089.

Ogawa, K., 2006. Stem respiration is influenced by pruning and girdling in Pinus sylvestris. Scand. J. For. Res. 21, 293–298. https://doi.org/10.1080/02827580600866188.

Öquist, M.G., He, H., Bortolazzi, A., Nilsson, M.B., Rodeghiero, M., Tognetti, R., Ventura, M., Egnell, G., 2024. Nitrogen fertilization increases N2O emission but does not offset the reduced radiative forcing caused by the increased carbon uptake in boreal forests. For. Ecol. Manage. 556 https://doi.org/10.1016/j.foreco.2024.121739.

Pan, Y., Birdsey, R.A., Fang, J., Houghton, R., Kauppi, P.E., Kurz, W.A., Phillips, O.L., Shvidenko, A., Lewis, S.L., Canadell, J.G., Ciais, P., Jackson, R.B., Pacala, S.W., McGuire, A.D., Piao, S., Rautiainen, A., Sitch, S., Hayes, D., 2011. A large and persistent carbon sink in the world's forests. Science 1979 (333), 988–993. https://doi.org/10.1126/science.1201609.

Pangala, S.R., Hornibrook, E.R.C., Gowing, D.J., Gauci, V., 2015. The contribution of trees to ecosystem methane emissions in a temperate forested wetland. Glob. Chang. Biol. 21, 2642–2654. https://doi.org/10.1111/gcb.12891.

Pangala, S.R., Enrich-Prast, A., Basso, L.S., Peixoto, R.B., Bastviken, D., Hornibrook, E.R. C., Gatti, L.V., Marotta, H., Calazans, L.S.B., Sakuragui, C.M., Bastos, W.R., Malm, O., Gloor, E., Miller, J.B., Gauci, V., 2017. Large emissions from floodplain trees close the Amazon methane budget. Nature 552, 230–234. https://doi.org/10.1038/nature24639.

Piñeiro, G., Perelman, S., Guerschman, J.P., Paruelo, J.M., 2008. How to evaluate models: observed vs. predicted or predicted vs. observed? Ecol. Model. 216, 316–322. https://doi.org/10.1016/j.ecolmodel.2008.05.006.

Pinheiro, J., Bates, D., 2023. nlme: Linear and Nonlinear Mixed Effects Models . R package version 3.1-162. Available at. https://CRAN.R-project.org/package=nlme.

Pitz, S., Megonigal, J.P., 2017. Temperate forest methane sink diminished by tree emissions. New Phytol. 214, 1432–1439. https://doi.org/10.1111/nph.14559.

Pitz, S.L., Megonigal, J.P., Chang, C.H., Szlavecz, K., 2018. Methane fluxes from tree stems and soils along a habitat gradient. Biogeochemistry 137, 307–320. https://doi.org/10.1007/s10533-017-0400-3.

Puhe, J., 2003. Growth and development of the root system of Norway spruce (Picea abies) in forest stands - a review. For. Ecol. Manage. 175, 253–273. https://doi.org/10.1016/S0378-1127(02)00134-2.

Putkinen, A., Siljanen, H.M.P., Laihonen, A., Paasisalo, I., Porkka, K., Tiirola, M., Haikarainen, I., Tenhovirta, S., Pihlatie, M., 2021. New insight to the role of microbes in the methane exchange in trees: evidence from metagenomic sequencing. New Phytol. 231, 524–536. https://doi.org/10.1111/nph.17365.

R Development Core Team, 2023. R: A Language and Environment for Statistical Computing. R Foundation for Statistical Computing, Vienna, Austria. Available at. http://www.R-project.org.

Ranniku, R., Schindler, T., Escuer-Gatius, J., Mander, Ü., Machacova, K., Soosaar, K., 2023. Tree stems are a net source of CH4 and N2O in a hemiboreal drained peatland forest during the winter period. Environ Res Commun 5, 051010. https://doi.org/10.1088/2515-7620/acd7c7.

Rusch, H., Rennenberg, H., 1998. Black alder (Alnus Glutinosa (L.) Gaertn.) trees mediate methane and nitrous oxide emission from the soil to the atmosphere. Plant and Soil 201, 1–7. https://doi.org/10.1023/A:1004331521059.

Ryan, M.G., Lavigne, M.B., Grower, S.T., 1997. Annual carbon cost of autotrophic respiration in boreal forest ecosystems in relation to species and climate. J. Geophys. Res. 102, 28871–28883. https://doi.org/10.1029/97JD01236.

Sakabe, A., Takahashi, K., Azuma, W., Itoh, M., Tateishi, M., Kosugi, Y., 2021. Controlling factors of seasonal variation of stem methane emissions from Alnus japonica in a riparian wetland of a temperate forest. J. Geophys. Res. Biogeosci. 126, e2021JG006326 https://doi.org/10.1029/2021JG006326.

Saunois, M., R. Stavert, A., Poulter, B., Bousquet, P., G. Canadell, J., B. Jackson, R., A. Raymond, P., J. Dlugokencky, E., Houweling, S., K. Patra, P., Ciais, P., K Arora, V., Bastviken, D., Bergamaschi, P., R. Blake, D., Brailsford, G., Bruhwiler, L., M. Carlson, K., Carrol, M., Castaldi, S., Chandra, N., Crevoisier, C., M. Crill, P.,

Covey, K., L. Curry, C., Etiope, G., Frankenberg, C., Gedney, N., I. Hegglin, M., Höglund-Isaksson, L., Hugelius, G., Ishizawa, M., Ito, A., Janssens-Maenhout, G., M. Jensen, K., Joos, F., Kleinen, T., B. Krummel, P., L. Langenfelds, R., G. Laruelle, G., Liu, L., MacHida, T., Maksyutov, S., C. McDonald, K., McNorton, J., A. Miller, P., R. Melton, J., Morino, I., Müller, J., Murguia-Flores, F., Naik, V., Niwa, Y., Noce, S., O'Doherty, S., Parker, R., Peng, C., Peng, S., P. Peters, G., Prigent, C., Prinn, R., Ramonet, M., Regnier, P., J. Riley, W., A. Rosentreter, J., Segers, A., J. Simpson, I., Shi, H., J. Smith, S., Paul Steele, L., F. Thornton, B., Tian, H., Tohjima, Y., N. Tubiello, F., Tsuruta, A., Viovy, N., Voulgarakis, A., S. Weber, T., Van Weele, M., R. Van Der Werf, G., F. Weiss, R., Worthy, D., Wunch, D., Yin, Y., Yoshida, Y., Zhang, W., Zhang, Z., Zhao, Y., Zheng, B., Zhu, Qing, Zhu, Qiuan, Zhuang, Q., 2020. The global methane budget 2000–2017. Earth Syst Sci Data 12, 1561–1623. https://doi.org/10.5194/essd-12-1561-2020.

Schindler, T., Mander, Ü., Machacova, K., Espenberg, M., Krasnov, D., Escuer-Gatius, J., Veber, G., Pärn, J., Soosaar, K., 2020. Short-term flooding increases CH4 and N2O emissions from trees in a riparian forest soil-stem continuum. Sci. Rep. 10, 3204. https://doi.org/10.1038/s41598-020-60058-7.

Schindler, T., Machacova, K., Mander, Ü., Escuer-Gatius, J., Soosaar, K., 2021. Diurnal tree stem CH4 and N2O flux dynamics from a riparian alder forest. Forests 12, 863. https://doi.org/10.3390/f12070863.

Shibistova, O., Lloyd, J., Zrazhevskaya, G., Arneth, A., Kolle, O., Knohl, A., Astrakhantceva, N., Shijneva, I., Schmerler, J., 2002. Annual ecosystem respiration budget for a Pinus sylvestris stand in central Siberia. Tellus B: Chemical and Physical Meteorology 54, 568–589. https://doi.org/10.3402/tellusb.v54i5.16688.

Silverthorn, T.K., Richardson, J.S., 2021. Temporal and microtopographical variations in greenhouse gas fluxes from riparian forest soils along headwater streams. Biogeochemistry 155, 401–412. https://doi.org/10.1007/s10533-021-00832-5.

Sjögersten, S., Siegenthaler, A., Lopez, O.R., Aplin, P., Turner, B., Gauci, V., 2020. Methane emissions from tree stems in neotropical peatlands. New Phytol. 225, 769–781. https://doi.org/10.1111/nph.16178.

Stockfors, J., Linder, S., 1998. Effect of nitrogen on the seasonal course of growth and maintenance respiration in stems of Norway spruce trees. Tree Physiol. 18, 155–166. https://doi.org/10.1093/treephys/18.3.155.

Sundqvist, E., Crill, P., Mölder, M., Vestin, P., Lindroth, A., 2012. Atmospheric methane removal by boreal plants. Geophys. Res. Lett. 39, L21806 https://doi.org/10.1029/2012GL053592.

Tarvainen, L., Wallin, G., Lim, H., Linder, S., Oren, R., Löfvenius, M.O., Räntfors, M., Tor-Ngern, P., Marshall, J., 2018. Photosynthetic refixation varies along the stem and reduces CO2 efflux in mature boreal Pinus sylvestris trees. Tree Physiol. 38, 558–569. https://doi.org/10.1093/treephys/tpx130.

Tenhovirta, S.A.M., Kohl, L., Koskinen, M., Patama, M., Lintunen, A., Zanetti, A., Lilja, R., Pihlatie, M., 2022. Solar radiation drives methane emissions from the shoots of Scots pine. New Phytol. 235, 66–77. https://doi.org/10.1111/nph.18120.

Terazawa, K., Yamada, K., Ohno, Y., Sakata, T., Ishizuka, S., 2015. Spatial and temporal variability in methane emissions from tree stems of Fraxinus mandshurica in a cool-temperate floodplain forest. Biogeochemistry 123, 349–362. https://doi.org/10.1007/s10533-015-0070-y.

Terazawa, K., Tokida, T., Sakata, T., Yamada, K., Ishizuka, S., 2021. Seasonal and weather-related controls on methane emissions from the stems of mature trees in a cool-temperate forested wetland. Biogeochemistry 156, 211–230. https://doi.org/10.1007/s10533-021-00841-4.

Teskey, R.O., Saveyn, A., Steppe, K., McGuire, M.A., 2008. Origin, fate and significance of CO2 in tree stems. New Phytol. 177, 17–32. https://doi.org/10.1111/j.1469-8137.2007.02286.x.

Tockner, K., Stanford, J.A., 2002. Riverine flood plains: present state and future trends. Environ. Conserv. 29, 308–330. https://doi.org/10.1017/S037689290200022X.

Vainio, E., Haikarainen, I.P., Machacova, K., Putkinen, A., Santalahti, M., Koskinen, M., Fritze, H., Tuomivirta, T., Pihlatie, M., 2022. Soil-tree-atmosphere CH4 flux dynamics of boreal birch and spruce trees during spring leaf-out. Plant and Soil 478, 391–407. https://doi.org/10.1007/s11104-022-05447-9.

Vidon, P., Allan, C., Burns, D., Duval, T.P., Gurwick, N., Inamdar, S., Lowrance, R., Okay, J., Scott, D., Sebestyen, S., 2010. Hot spots and hot moments in riparian zones: potential for improved water quality management. J. Am. Water Resour. Assoc. 46, 278–298. https://doi.org/10.1111/j.1752-1688.2010.00420.x.

Vigano, I., Van Weelden, H., Holzinger, R., Keppler, F., Mcleod, A., Röckmann, T., 2008. Effect of UV radiation and temperature on the emission of methane from plant biomass and structural components. Biogeosciences 5, 937–947. https://doi.org/10.5194/bg-5-937-2008.

Wang, Z.P., Gu, Q., Deng, F.D., Huang, J.H., Megonigal, J.P., Yu, Q., Lü, X.T., Li, L.H., Chang, S., Zhang, Y.H., Feng, J.C., Han, X.G., 2016. Methane emissions from the trunks of living trees on upland soils. New Phytol. 211, 429–439. https://doi.org/10.1111/nph.13909.

Wang, Z.P., Han, S.J., Li, H.L., Deng, F.D., Zheng, Y.H., Liu, H.F., Han, X.G., 2017. Methane production explained largely by water content in the heartwood of living trees in upland forests. J. Geophys. Res. Biogeosci. 122, 2479–2489. https://doi.org/10.1002/2017JG003991.

Wen, Y., Corre, M.D., Rachow, C., Chen, L., Veldkamp, E., 2017. Nitrous oxide emissions from stems of alder, beech and spruce in a temperate forest. Plant and Soil 420, 423–434. https://doi.org/10.1007/s11104-017-3416-5.

Yip, D.Z., Veach, A.M., Yang, Z.K., Cregger, M.A., Schadt, C.W., 2019. Methanogenic Archaea dominate mature heartwood habitats of Eastern Cottonwood (Populus deltoides). New Phytol. 222, 115–121. https://doi.org/10.1111/nph.15346.

Yvon-Durocher, G., Allen, A.P., Bastviken, D., Conrad, R., Gudasz, C., St-Pierre, A., Thanh-Duc, N., del Giorgio, P.A., 2014. Methane fluxes show consistent temperature dependence across microbial to ecosystem scales. Nature 507, 488–491. https://doi.org/10.1038/nature13164.

Zeikus, J.G., Ward, J.C., 1974. Methane formation in living trees: a microbial origin. Science 1979 (184), 1181–1183. https://doi.org/10.1126/science.184.4142.1181.

Zhao, J., 2019. FluxCalR: a R package for calculating CO2 and CH4 fluxes from static chambers. JOSS. The Journal of Open Source Software 4, 1751. https://doi.org/10.21105/joss.01751.

Zuur, A., Ieno, E.N., Walker, N., Saveliev, A.A., Smith, G.M., 2009. Mixed Effects Models and Extensions in Ecology With R. Springer.